

Pyrido[2,3-*d*]pyrimidin-5-ones: A Novel Class of Antiinflammatory Macrophage Colony-Stimulating Factor-1 Receptor Inhibitors[†]

Hui Huang, Daniel A. Hutta, James M. Rinker, Huaping Hu, William H. Parsons, Carsten Schubert, Renee L. DesJarlais, Carl S. Cryslar, Margery A. Chaikin, Robert R. Donatelli, Yanmin Chen, Deping Cheng, Zhao Zhou, Edward Yurkow, Carl L. Manthey, and Mark R. Player*

Johnson & Johnson Pharmaceutical Research and Development, Welsh and McKean Roads, Spring House, Pennsylvania 19477-0776

Received November 7, 2008

A series of pyrido[2,3-*d*]pyrimidin-5-ones has been synthesized and evaluated as inhibitors of the kinase domain of macrophage colony-stimulating factor-1 receptor (FMS). FMS inhibitors may be useful in treating rheumatoid arthritis and other chronic inflammatory diseases. Structure-based optimization of the lead amide analogue **10** led to hydroxamate analogue **37**, which possessed excellent potency and an improved pharmacokinetic profile. During the chronic phase of streptococcal cell wall-induced arthritis in rats, compound **37** (10, 3, and 1 mg/kg) was highly effective at reversing established joint swelling. In an adjuvant-induced arthritis model in rats, **37** prevented joint swelling partially at 10 mg/kg. In this model, osteoclastogenesis and bone erosion were prevented by low doses (1 or 0.33 mg/kg) that had minimal impact on inflammation. These data underscore the potential of FMS inhibitors to prevent erosions and reduce symptoms in rheumatoid arthritis.

Introduction

Macrophage colony-stimulating factor-1 receptor (FMS^a) (cellular homologue of the V-FMS oncogene product of the Susan McDonough strain of feline sarcoma virus) is a class III receptor tyrosine kinase and is the exclusive receptor for colony stimulating factor-1 (CSF-1).¹ CSF-1 is an important growth factor for bone progenitor cells, monocytes, macrophages,² and cells of macrophage lineage such as osteoclasts³ and dendritic cells.⁴ Binding of CSF-1 to the FMS extracellular domain induces FMS dimerization and trans-autophosphorylation of the intracellular FMS kinase domain on several tyrosine residues. Once phosphorylated, FMS serves as a docking site for several cytoplasmic signaling molecules the activation of which leads to de novo gene expression and proliferation.⁵ Robust expression of FMS is restricted to monocytes, tissue macrophages, and osteoclasts. For this reason it is anticipated that FMS inhibitors will be useful in treating diseases where osteoclasts, dendritic cells, and macrophages are pathogenic, e.g., rheumatoid arthritis (RA) and other autoimmune/inflammatory diseases.

Rheumatoid arthritis afflicts approximately 1% of the U.S. population and exacts a large personal and economic burden. It is an autoimmune disease, and several cartilage autoantigens have been proposed but none proven to drive pathogenesis. Acquired cellular and humoral immunity activates synovial tissue macrophages to express cytokines that further orchestrate leukocytic infiltration, edema, and pain. The synovial inflammation is chronic and eventually organizes to form granulation tissue known as a pannus. Pannus is a highly invasive tissue that progressively erodes cartilage, bone, tendons, and ligaments with irreversible loss of joint function, particularly of the hands and feet. Because of a generalized increase in inflammatory

mediators, RA also has systemic manifestations. RA patients have a greater incidence of vascular disease⁶ and osteoporosis.⁷ Although patients seek relief from pain and stiffness, new agents are needed that prevent progressive loss of joint function and reduce the manifestations of systemic disease.

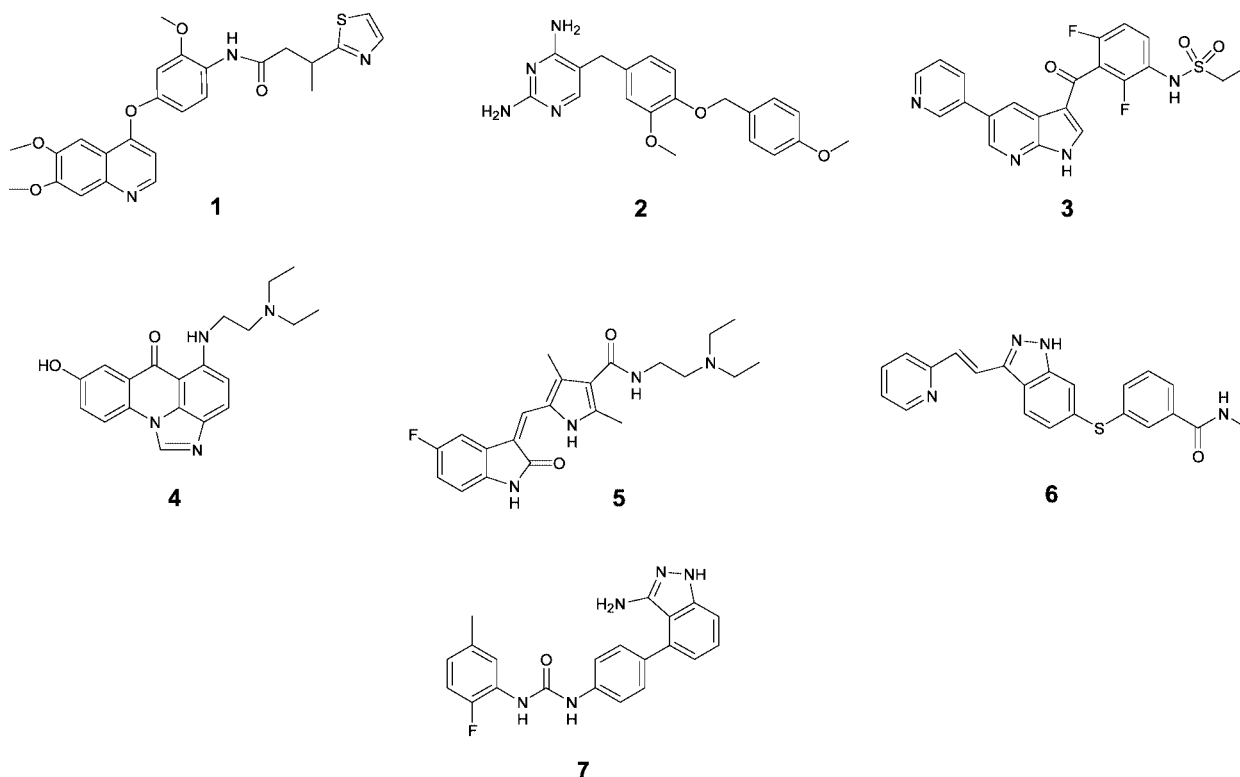
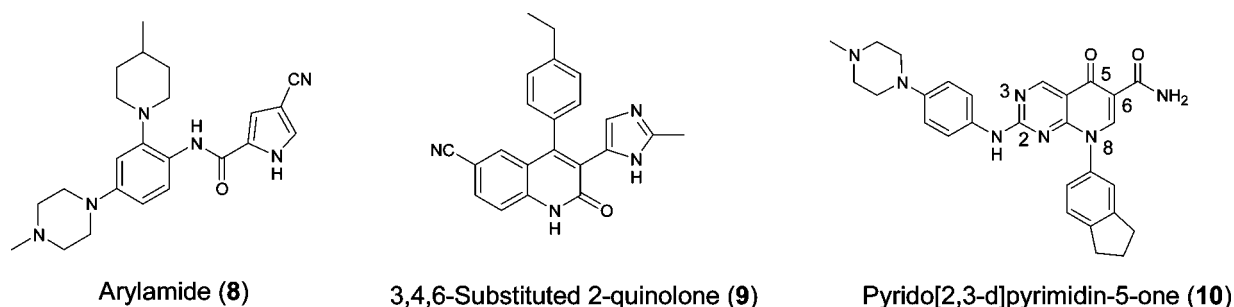
Low-dose methotrexate is the first-line therapy for moderate to severe RA. Although methotrexate is economical and has reduced a great deal of suffering, some 35–55% of patients fail to achieve (American College of Rheumatology-20) ACR20 response rates with methotrexate alone and methotrexate does not adequately control focal bone erosions and generalized osteoporosis in RA.⁸ Patients using methotrexate must be monitored closely for elevated liver enzymes to prevent liver fibrosis, and use of methotrexate is associated with transient nausea and fatigue in a majority of patients.⁹ Patients that do not respond adequately to methotrexate may be prescribed one of several biological agents that neutralize TNF (infliximab, etanercept, adalimumab, and abatacept) or CD20 (rituximab). These agents effectively reduce local and systemic symptoms and prevent joint space narrowing and bone erosions in the majority of patients. However, they are expensive and require parenteral administration. Thus, there remains an untapped market for an efficacious oral drug that is better tolerated than methotrexate, particularly one that protects the patient from joint destruction.

There is evidence that CSF-1 may drive the macrophage population in RA. CSF-1 levels are elevated in rheumatoid plasma, synovium, and synovial fluid.¹⁰ Monocytes from RA patients express elevated levels of FcγR I, IIa, and IIIa, increased CD14 and oxygen radicals, and reduced HLA-DR.¹¹ This monocyte phenotype can be produced in vitro and in vivo with recombinant CSF-1.¹² Thusly, CSF-1 may drive the recruitment, differentiation and survival of RA synovial macrophages, and the local proliferation of myeloid progenitors. Further, CSF-1 primes macrophages for greater expression of TNF and other cytokines.¹³ It has been proposed that CSF-1 is a component of a positive feedback loop in chronic inflammation.¹⁴ In this loop, macrophages secrete TNF and IL-1 that induce stromal

* To whom correspondence should be addressed. Phone: 610-458-6980. Fax: 610-458-6980. E-mail: mplayer@its.jnj.com.

[†] PDB ID: 3DPK.

^a Abbreviations: SCF, stem cell factor; FMS, macrophage colony-stimulating factor-1 receptor; ITD, internal tandem duplication; FLT-3, FMS-like tyrosine kinase-3; FCS, fetal calf serum; MEM, minimal essential media; RNase, ribonuclease; DNase, deoxyribonuclease; SEM, standard error of the mean.

Chart 1. FMS Inhibitors**Chart 2.** Three Novel Classes of FMS Inhibitors

cell expression of CSF-1, causing further expansion of macrophage numbers and increased TNF and IL-1 expression. Therapeutic targeting of TNF and IL-1 with biologic agents has been successful.¹⁵ Interruption of CSF-1 signaling with oral FMS inhibitors may provide a novel alternative approach to break the positive feedback loop in inflammatory disease. Further, because FMS was shown to mediate TNF-induced osteolysis,¹⁵ we anticipate that oral FMS inhibitors will be useful for preventing focal bone loss, deformity, and loss of joint function in rheumatoid arthritis.

There are a number of small molecule FMS inhibitors reported in the literature, such as **1** (Ki20227),¹⁶ **2** (GW2580),¹⁷ **3** (P-0728),¹⁸ **4** (XLS-002),¹⁹ **5** (sunitinib),²⁰ **6** (AG13736),²¹ and **7** (ABT869).²² While many of them have demonstrated in vivo antiinflammatory efficacy and are in various stages of development, **5–7** are multitargeted kinase inhibitors in clinical trials for cancer therapies (Chart 1).

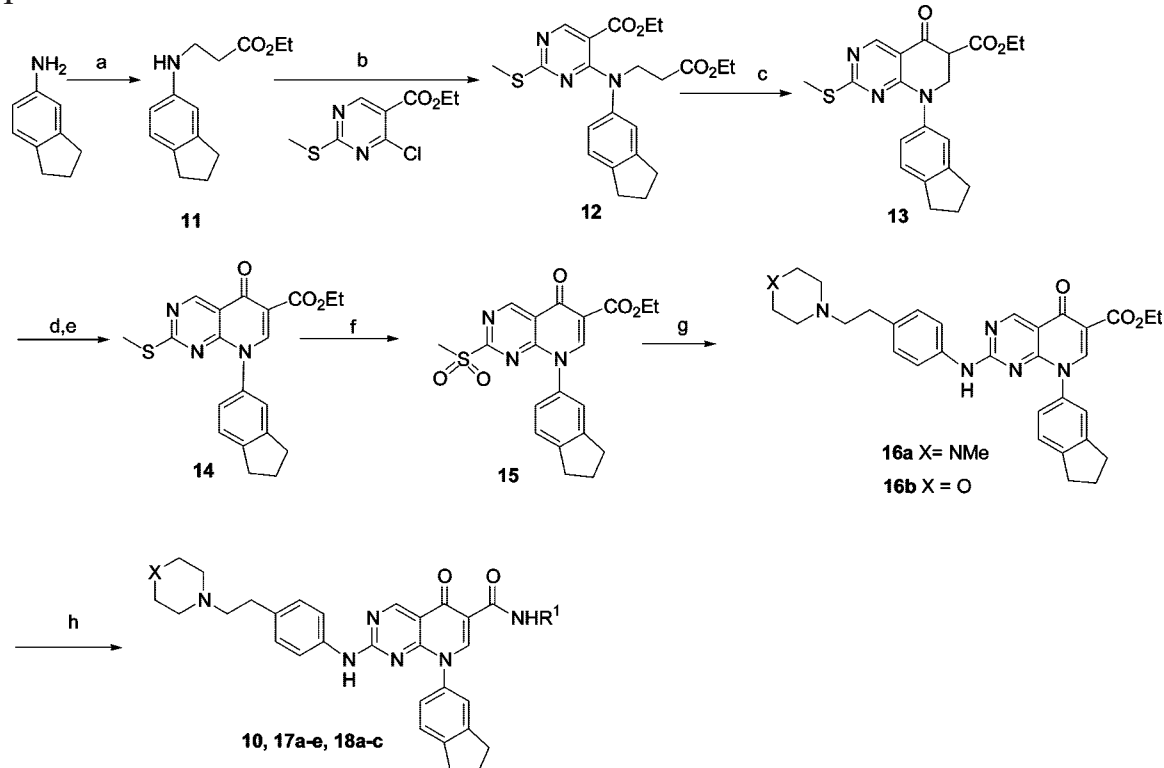
We have identified several classes of novel FMS inhibitors: arylamides (**8**),²³ 3,4,6-substituted 2-quinolones (**9**),²⁴ and pyrido[2,3-*d*]pyrimidin-5-ones (**10**),²⁵ which have good in vitro and in vivo activities (Chart 2). Herein is reported the structure-based optimization of the pyrido[2,3-*d*]pyrimidin-5-one core, which has led to FMS inhibitors with significantly improved

pharmacokinetic properties and potent anti-inflammatory efficacy in in vivo arthritis models.

Chemistry

The synthesis of pyrido[2,3-*d*]pyrimidin-5-one amide **10** is shown in Scheme 1. 5-Aminoindan was reacted with ethyl 3-chloropropionate at elevated temperature in the presence of an inorganic base and a catalytic amount of tetrabutylammonium bromide, affording the aminopropionate ester **11**. Compound **11** was then treated with ethyl 4-chloro-2-methylthio-5-pyrimidinecarboxylate to produce 4-aminopyrimidine **12**. Cyclization of this diester under Dieckmann conditions afforded bicyclic compound **13**. Subsequent halogenation with bromine followed by dehydrohalogenation gave **14**.²⁶ The thiomethyl moiety was then oxidized to sulfone **15**, which was subsequently displaced with an alkyl amine or aniline by nucleophilic substitution. The resulting carboxylate ester **16** was converted to amides **10**, **17a–e**, and **18a–c** by reaction with corresponding amines in methanol at elevated temperatures.

After the methyl hydroxamate group was shown to be optimal at the C-6 position (**18a**, Table 1, Scheme 1), an alternate route was developed in order to incorporate the methyl hydroxamate

Scheme 1^a

^a Reagents and conditions: (a) ethyl 3-chloropropionate, K₂CO₃, Bu₄NBr (cat.), 100 °C; (b) Et₃N, *n*-BuOH, rt; (c) *t*-BuONa, toluene, 90 °C; (d) Br₂, CH₂Cl₂, rt; (e) Et₃N, CH₂Cl₂, rt; (f) *m*-CPBA, CH₂Cl₂, rt; (g) arylamine, *i*-PrOH, 90 °C; (h) R¹NH₂, MeOH, rt or 80–100 °C.

Table 1. Effect of C-6 Amide Substitution on Biological Activity and Rat Liver Microsomal Stability

compd	R ¹	X	FMS enzyme IC ₅₀ ^a (nM)	BMDM IC ₅₀ ^b (nM)	RLM stability ^c
10			13	16	87
17a	H	NCH ₃	0.8	9	96
17b	Me	NCH ₃	1.2	26	73
17c	Me	O	1.4	55	100
17d	Et	NCH ₃	3.2	45	ND ^d
17e	CH ₂ CH ₂ OH	NCH ₃	0.7	56	84
18a	OMe	NCH ₃	0.7	1.3	78
18b	OEt	NCH ₃	0.5	3.3	84
18c	OCH(CH ₃) ₂	NCH ₃	0.5	5.4	100

^a Reported IC₅₀ values are means of three experiments. Interassay variance was <10%. ^b Dose–response data are the average of at least two replicates per dose. ^c Percentage of compound remaining after 10 min incubation in rat liver microsomes. ^d Not determined.

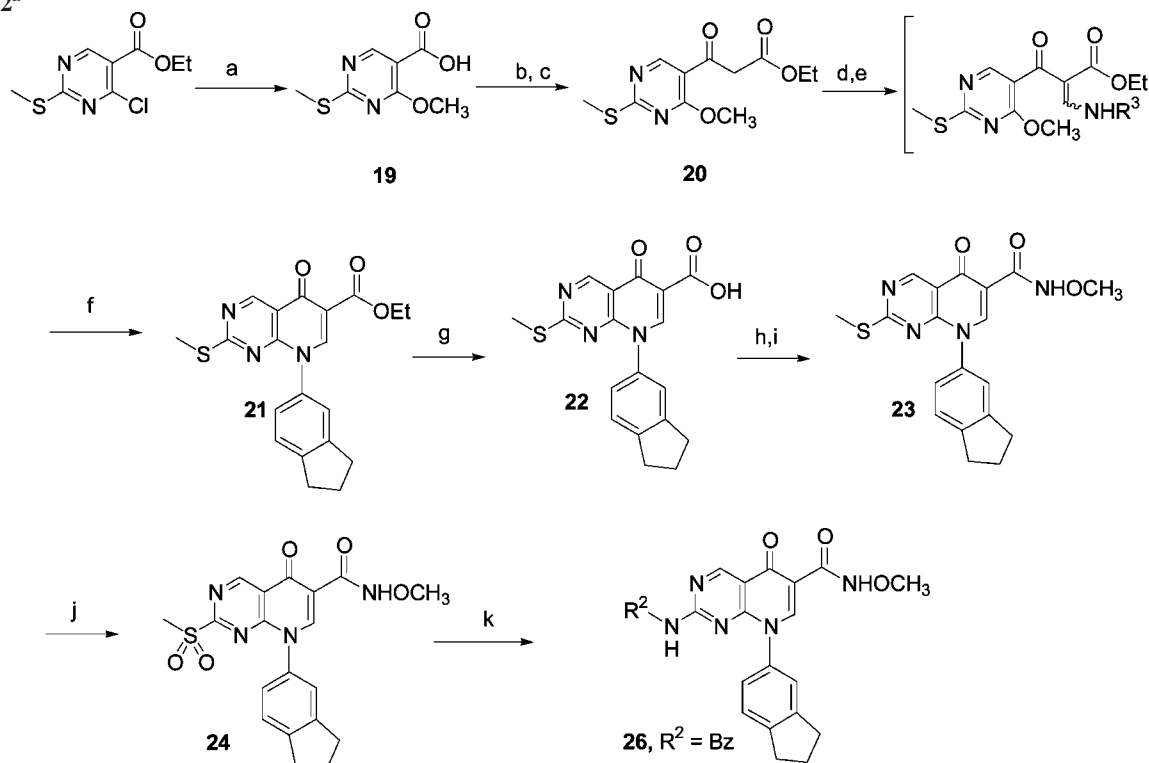
group earlier in the synthetic sequence (Scheme 2). Ethyl 4-chloro-2-methylthio-5-pyrimidinecarboxylate was saponified to the corresponding acid **19**. The 4-chloride was displaced by a methoxyl group under the conditions noted. However, the methoxyl group was found to serve the same role as the chloride in subsequent steps. Ketoester **20**, prepared from an acid chloride intermediate, was converted to an enaminoester intermediate by reaction with ethyl orthoformate and acetic anhydride, followed by reaction with a primary amine R³NH₂.²⁷ A base-assisted cyclization reaction of the unisolated enaminoester

led to bicyclic ester **21**. Acid **22**, obtained through acidic hydrolysis of **21**, was coupled with methoxyamine to form **23**. The 2-methylthio group of **23** was oxidized to give methylsulfone **24**, which was subsequently displaced with anilines R²NH₂ to give final products. This route allowed rapid exploration of the C-2 anilino substituents and facilitated evaluation of N-8 substitutions using common intermediate **20**.

Results and Discussion

As previously reported, pyrido[2,3-*d*]pyrimidin-5-one **10** was a potent FMS inhibitor with an IC₅₀ of 13 nM.²⁵ Further optimization of the C-2 anilino substituents led to **17a** with improved potency in the enzyme assay²⁸ and in the cellular assay that measures proliferation of bone marrow-derived macrophages (BMDM)²⁹ in response to CSF-1 stimulation (Table 1). Small alkyl substitution on the C-6 amide was well tolerated, though activity diminished with increasing size (**17b,d**). Despite good in vitro activity, the amide series (**10**, **17a**, and **17c**) exhibited poor oral exposure when administered at 10 mg/kg to male Sprague–Dawley rats (Table 2). Moreover, these compounds showed high volumes of distribution and high clearance rates. Because the amide series was stable in rat liver microsomal (RLM) incubations, the lack of oral exposure was suspected to be a result of poor absorption.

The cocrystal structure of an amide compound bound in the active site of FMS revealed that the amide NH is part of a water-mediated hydrogen bonding network.²⁵ It was hypothesized that displacing the water molecule and preserving the hydrogen bonding network might improve potency. Molecular modeling suggested that 2-hydroxyethyl amide (**17e**) had the potential to achieve this. Compound **17e** was potent in the enzyme assay but substantially less active than the corresponding amide **17a** in the BMDM assay. Alkyl hydroxamates (**18a–c**) were also designed to explore this hypothesis. The hydroxamate group

Scheme 2^a

^a Reagents and conditions: (a) NaOH, methanol, rt; (b) oxalyl chloride, DMF (cat.), CH₂Cl₂, 0 °C to rt; (c) ethyl hydrogen malonate, MeMgBr, 0 °C to rt; (d) triethylorthoformate, Ac₂O, 130 °C; (e) aminoindan, THF, rt; (f) K₂CO₃, THF, rt; (g) 1 N HCl, 1,4-dioxane, 105 °C; (h) oxalyl chloride, DMF (cat.), CH₂Cl₂, 0 °C to rt; (i) methoxyamine hydrochloride, Et₃N, CH₂Cl₂, 0 °C to rt; (j) *m*-CPBA, CH₂Cl₂, rt; (k) R²NH₂, AcOH, 110 °C.

Table 2. Pharmacokinetic Profile of Selected Analogues in Sprague–Dawley Rats

compd ^a	C _{max} po ^b (μM)	t _{1/2} po (h)	t _{1/2} iv (h)	Cl (mL/min/kg)	Vd _{ss} ^d (L/kg)	F (%)
10				133	18.7	0
17a			7	25	15.5	0
17c	0.13	1.8	0.7	47	2.6	4
18a	2.7	6.5	4.5	4	1.5	57
31	0.08	9.7	6	10	0.8	3
35	0.13		3	34	8.8	8
36			1.7	38	5.1	0
37	1.6	6.9	4.6	11	4.3	100
39	0.4		5.2	20.4	5.6	28
45	3.4	8.1	8	8	5.9	103

^a Formulated in 20% hydroxypropyl-β-cyclodextrin (HPβCD). ^b Administered at 10 mg/kg po. ^c Administered at 2 mg/kg iv. ^d Volume of distribution at steady state. Both Cl and Vd determined from iv dosing.

presents a distinct electrostatic surface for interaction and was expected to displace one of the bound water molecules. Methyl hydroxamate **18a** exhibited significantly increased potency in the BMDM assay while retaining the enzyme activity of the amide **17a**. Furthermore, **18a** had an improved pharmacokinetic profile in rat with an oral bioavailability of 57%, a C_{max} of 2.7 μM at a 10 mg/kg oral dose, and a low systemic clearance rate (4 mL/min/kg) (Table 2). Small alkyl hydroxamates were all potent FMS inhibitors, although BMDM activity decreased with increasing size of the alkyl group (**18b,c**). Some of these analogues have kinase assay IC₅₀s around the enzyme concentration of 0.9 nM. As enzyme activity approached this limit, the BMDM cell-based assay was more sensitive to differences in potency.

Subsequently, one of the methyl hydroxamates (**25**) was cocrystallized with FMS (Figure 1). Like previously analyzed FMS inhibitors,^{25,30} the hydroxamate series interacts with the hinge region of the kinase via hydrogen bonding interactions

mediated through the C-2 anilino NH and the pyrimidine N-3 (Figure 1A). A water-mediated hydrogen bonding network is formed between the C-5 carbonyl oxygen, the hydroxyl group of Thr663 and a water molecule present in the active site (Figure 1B). The hydroxamate group preserves the conformational constraint of the intramolecular hydrogen bond between the NH and C-5 carbonyl oxygen. This in turn enables the acetamide carbonyl to interact with Lys616. In addition, the hydroxamate oxygen forms hydrogen bonds with Lys616. It is believed that this complex hydrogen bonding network contributes to the improved potency.

The importance of the aromatic nature of the C-2 substituents is evident, given that compounds with alkyl amino substitutions at C-2 position (**26**, **27**) had poor activity (Table 3). The cocrystal structure of **25** bound in FMS shows that the pocket for C-2 substitution is quite narrow and cannot accommodate alkyl groups that would have a significant out-of-plane geometry. Crystal structures also predict that the substitution at the 4-position of the C-2 anilino phenyl ring would be solvent exposed. This region of the molecule has been used to modulate various properties of the compound while maintaining potent FMS inhibition.

To assess the specificity profile of FMS inhibitors as the program progressed, compounds were routinely assessed in a 50-assay counterscreening profile (GPCRs, ion channels, and transporters) at Cerep.³¹ In this screen, compound **18a** inhibited 16 targets by 50% or more at a concentration of 10 μM. In contrast, compounds with less basic substituents on the C-2 anilino phenyl inhibited fewer targets (data not shown). Therefore, efforts refocused on replacement of the basic piperazine tail of **18a**. At first, piperazine was replaced by less basic rings such as morpholine (**29**), 4,4-difluoropiperazine (**30**), and piperazin-2-one (**31**) (Table 3). Morpholino analogue **29** was more potent than its amide counterpart **17c** but was unstable

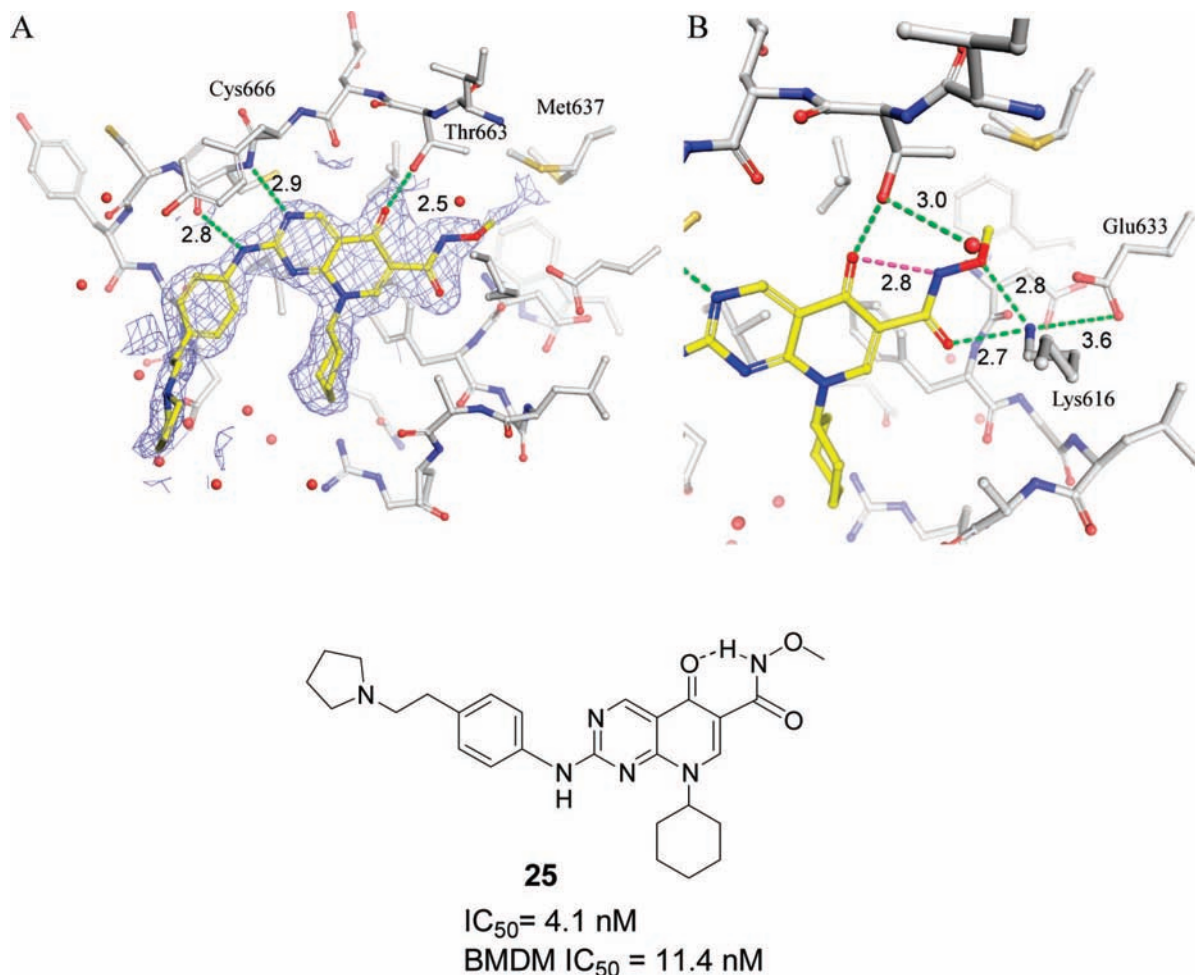


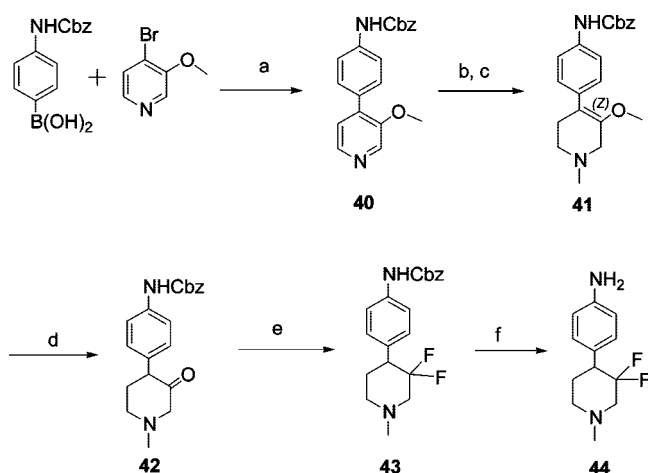
Figure 1. Cocystal structure of **25** in FMS (PDB ID: 3DPK). (A) Ball-and-stick representation of **25** (yellow) bound in the active site of cFMS (gray). Additionally shown is the $2f_o - f_c$ electron density map (blue) contoured at 1.4σ and truncated to a radius of 2 Å beyond each atom for clarity. Hydrogen bonds to the backbone of the protein are depicted as green dashed lines. (B) Close-up view of the water-mediated hydrogen-bonding network in the active site. The internal hydrogen bond between the amide nitrogen and the pyridopyrimidinone carbonyl oxygen is drawn in magenta.

in human and rat liver microsomes. While stable in HLM and RLM and clean in the counterscreening profile, the difluorinated piperidine analogue (**30**) was less active in the BMDM assay. Piperazin-2-one analogue (**31**) also exhibited a clean counterscreening profile, confirming the refocused strategy. However,

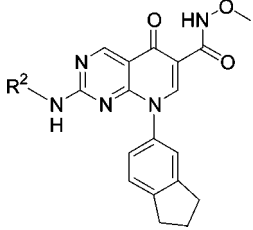
its oral bioavailability in rat was only 3% (Table 2). Methylated analogue **32** was prepared in an attempt to improve on the permeability of **31**, but it decomposed rapidly in HLM incubations. Neutral and acidic compounds were also prepared and had clean counterscreening profiles. However, it was difficult to formulate the neutral compounds for in vivo assessment due to poor solubility. Incorporation of acidic “tails” resulted in loss of activity in the BMDM assay, as seen in acetyl sulfonamide **33**.

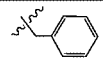
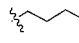
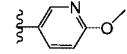
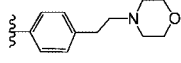
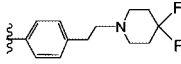
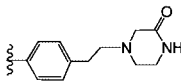
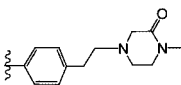
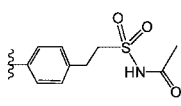
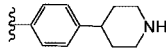
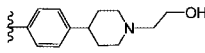
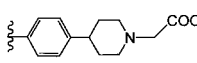
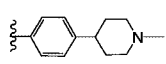
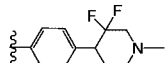
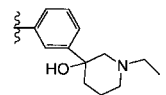
The ethyl linker was removed to give piperidine analogues **34–37**. Compound **34** was as potent as **18a** and had a similar counterscreening profile. Introduction of a hydroxyl ethyl group (**35**) had minimal impact on the potency, while acetic acid analogue (**36**) reduced BMDM activity more than 20-fold compared to **34** (Table 3). Both **35** and **36** had very low oral exposure in rat (Table 2). The *N*-methylated piperidine analogue (**37**) stood out not only for its excellent potency, but also for its good rat pharmacokinetic profile with an oral C_{max} of 1.6 μM , a clearance rate of 11 mL/min/kg, and bioavailability of 100% (Table 2). Although **37** was not optimal in the counterscreening profile as measured by inhibition of paradigm assays showed that hM1 was the only target where modest functional activity was observed.

Scheme 3^a



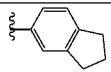
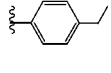
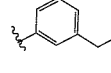
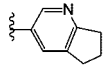
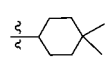
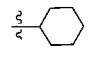
^a Reagents and conditions: (a) $\text{Pd}(\text{PPh}_3)_4$, Na_2CO_3 , toluene, ethanol, 110 °C; (b) MeI, acetone, 50 °C; (c) NaBH_4 , 0 °C to rt; (d) 6 N HCl, THF, 60 °C; (e) Deoxo-Fluor, CH_2Cl_2 , 0 °C to rt; (f) H_2 , Pd/C, methanol, rt.

Table 3. Effect of C-2 Substitution on Biological Activity and Rat/Human Liver Microsomal Stability


Cmpd	R ²	FMS Enzyme	BMDM	HLM	RLM
		IC ₅₀ ^a (nM)	IC ₅₀ ^b (nM)	stability ^c	Stability ^d
26		75	>300	N.D.	N.D.
27		15	>300	N.D.	N.D.
28		5.2	84	N.D.	N.D.
29		1.3	0.9	5.2	24
30		1.7	12	83	86
31		0.8	2.1	35	69
32		0.8	2.4	2.8	29
33		2.4	100	84	83
34		0.5	1.1	97	93
35		1.3	1	80	100
36		2.2	23	100	99
37		0.4	0.6	87	96
38		0.7	2	16	44
39		0.8	0.7	88	89

^a Reported IC₅₀ values are means of three experiments. Interassay variance was <10%. ^b Dose-response data are the average of at least two replicates per dose. ^c Percentage of compound remaining after 10 min incubation in human liver microsomes. ^d Percentage of compound remaining after 10 min incubation in rat liver microsomes.

Table 4. Effect of N-8 Substitution on Biological Activity and Rat/Human Liver Microsomal Stability

Cmpd	R ³	FMS Enzyme IC ₅₀ ^a (nM)	BMDM IC ₅₀ ^b (nM)	HLM stability ^c	RLM stability ^d
37		0.4	0.6	87	96
45		0.3	0.6	75	96
46		0.4	2	N.D.	N.D.
47		7	130	N.D.	N.D.
48		0.4	1	93	97
49		5	2.5	96	68

^a Reported IC₅₀ values are means of three experiments. Interassay variance was <10%. ^b Dose-response data are the average of at least two replicates per dose. ^c Percentage of compound remaining after 10 min incubation in human liver microsomes. ^d Percentage of compound remaining after 10 min incubation in rat liver microsomes.

Table 5. Kinase Selectivity of Selected Compounds

kinase ^a	17a (μM) ^b	18a (μM)	36 (μM)	37 (μM)
FMS	0.0008	0.0007	0.0022	0.0004
FLT3	0.001	0.036	0.041	0.006
KIT	0.020	0.006	0.013	0.006
PDGFR-β	>42	5.3	>2	0.15
Axl	>0.5	>0.5	>0.5	>1
TrkA	0.17	>0.5	>0.5	0.5
IRK-β	>42	19.8	9.3	3.7
Src	5.9	1.5	0.93	1.4

^a IC₅₀ values were determined at the respective ATP K_m of each kinase.

^b IC₅₀ values are means of three experiments. Interassay variance was <10%.

Table 6. Pharmacokinetic Profiles of **37** in Multiple Species

species ^a	C _{max} po (μM)	t _{1/2} po (h)	t _{1/2} iv (h)	Cl (mL/min/kg)	Vd _{ss} (L/kg)	F (%)
rat	1.6	6.9	4.6	11	4.3	100
mouse	0.9	4	1.8	34	3.6	51
dog	0.12		9.3	30	20.3	33
monkey	0.06		6.6	48.7	22.6	16.7

^a Administrated at 10 mg/kg po, 2 mg/kg iv for all species in 20% hydroxypropyl-β-cyclodextrin (HPβCD).

In an effort to attenuate basicity of the piperidine ring, difluoro-substituted piperidine analogue **38** and 3-hydroxyl piperidine analogue **39** were prepared. The aniline precursor of **38**, 4-(3,3-difluoro-1-methyl-piperidin-4-yl)-phenylamine (**44**) was synthesized as shown in Scheme 3. Suzuki coupling of the boronic acid with 3-methoxy-4-bromopyridine provided biaryl

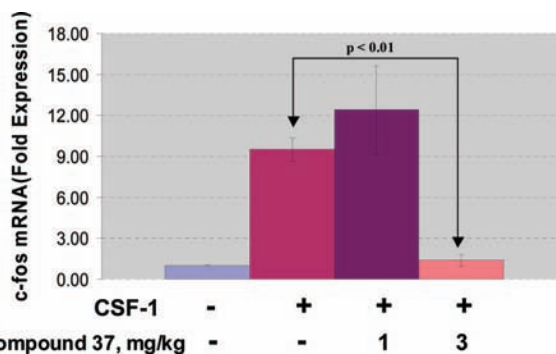


Figure 2. In vivo inhibition of FMS 6 h after dosing mice with **37**. B6C3R1 mice were dosed orally with **37** 6 h prior to a tail-vein injection of 1 μg recombinant CSF-1. Fifteen minutes following the CSF-1 challenge, mice were sacrificed and the functional status of FMS signaling was assessed by assay of c-fos mRNA in spleens as described in the Experimental Section.

40. It was then converted to the corresponding *N*-methyl pyridinium salt, followed by borohydride reduction to give tetrahydropyridine **41**.³² Acidic treatment of **41** gave 1-methylpiperid-3-one **42**, which was subsequently treated with bis-(2-methoxyethyl)aminosulfur trifluoride to give 3,3-difluoro-substituted piperidine **43**. Hydrogenolytic deprotection of the Cbz group provided the aniline **44**. The electron withdrawing effect of the difluoro group of **38** did not affect FMS activity

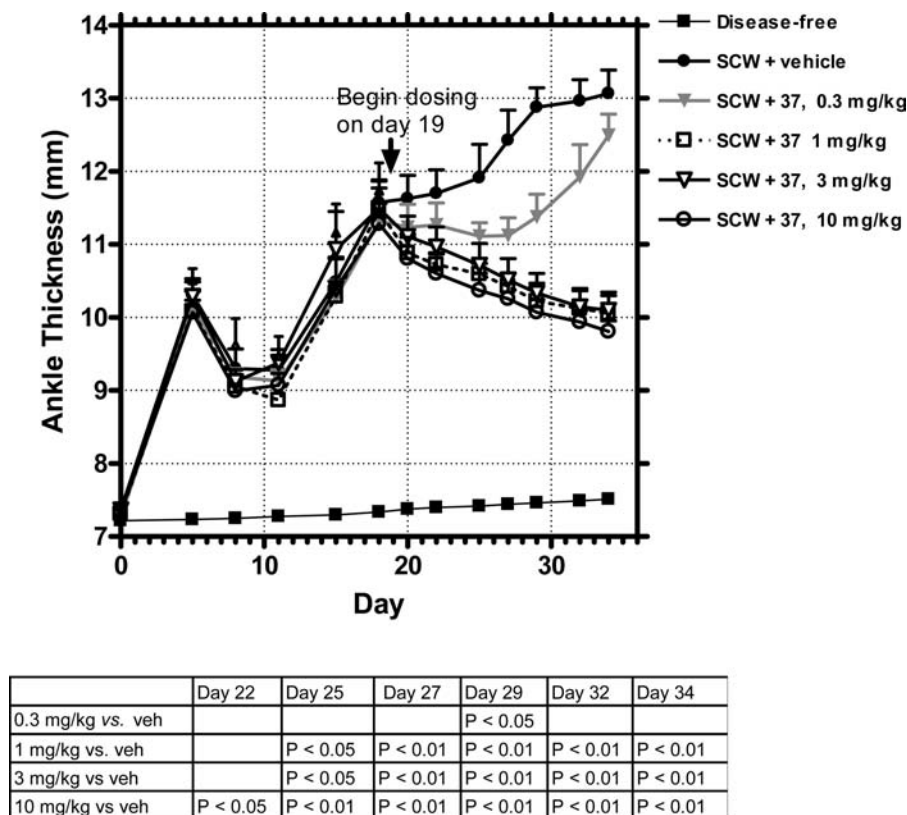


Figure 3. Compound 37 reversed ankle swelling during the chronic phase of SCW-induced arthritis. Arthritis was induced in rats by a single ip injection of SCW on day 0. Twice daily oral dosing with vehicle or 37 was commenced on day 19 when chronic inflammation was well established. Ankle thickness was measured using calipers as described in the Experimental Section.

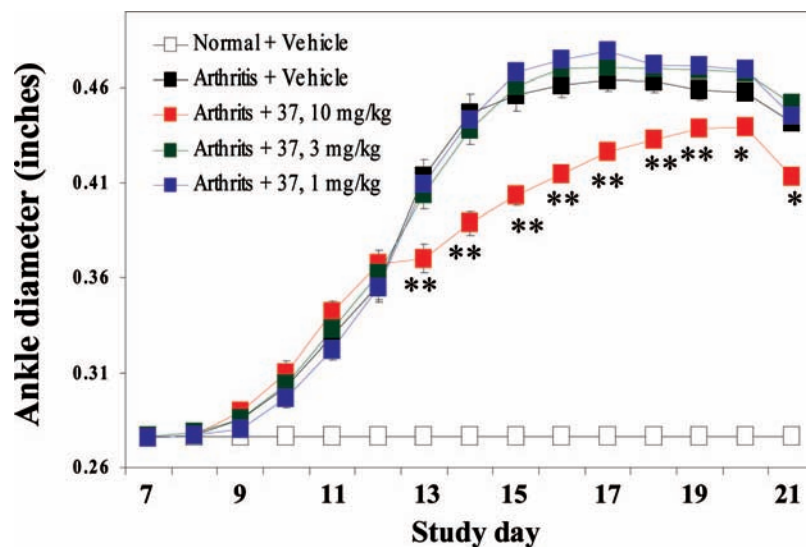


Figure 4. Compound 37 reduced paw swelling in adjuvant-induced arthritis. Adjuvant arthritis was induced in rats as described in the Experimental Section. Twice daily oral dosing with vehicle or 37 was commenced on day 8. Calipers were used to measure ankle thickness daily (mean \pm SEM). ** p < 0.001, * p < 0.01 vs arthritis + vehicle.

but resulted in poor solubility and low liver microsomal stability (Table 3). Compounds containing 1,3-substitution patterns on the C-2 aniline were also explored (39) and were potent FMS inhibitors. However, 39 demonstrated a C_{\max} of only 0.4 μ M after oral administration in rat and had a moderate clearance rate (20 mL/min/kg) (Table 2).

Having identified the *N*-methylpiperidine tail as an optimal C-2 substitution, N-8 substitution was next investigated (Table 4). When bound to FMS, N-8 substituents occupy a hydrophobic pocket, which can accommodate a variety of aromatic (37,

45–47) or aliphatic rings (25, 48–49). The 4-ethylphenyl analogue 45 was equipotent to indan analogue 37 and had a slightly improved rat pharmacokinetic profile compared to 37 in terms of oral exposure and clearance rate (Table 2). The 3-ethylphenyl analogue 46 was comparable to 37 and 45 in activity. The loss in activity by incorporation of nitrogen into the indan phenyl ring (47) confirmed the importance of hydrophobic substitution at the N-8 position. Aliphatic rings were well tolerated, and the bulkier dimethyl cyclohexyl analogue 48 was more potent than the cyclohexyl analogue 49.

Table 7. Effect of **37** on Swelling, Bone Erosion, and Osteoclast Counts in Adjuvant Arthritis

treatment	percent inhibition of ankle swelling, AUC	bone erosion score ^a	osteoclast counts ^b
Experiment no. 1 ^c			
vehicle (20% HPβCD)		4.88 (0.41)	29.3 (5.2)
37 , 1 mg/kg	−0.9	0.6 (0.6)**	0.2 (0.1)**
37 , 3 mg/kg	−0.9	0 (0)**	0.1 (0.1)**
37 , 10 mg/kg	17*	0 (0)**	0 (0)**
Experiment no. 2 ^c			
vehicle (20% HPβCD)		4.25 (0.41)	29.9 (3.2)
37 , 0.33 mg/kg	7	1.88 (0.23)**	9.9 (2.4)*
37 , 1 mg/kg	2	0 (0)**	0 (0)**
37 , 3 mg/kg	8	0 (0)**	0 (0)**

^a Based on microscopic examination of H and E stained sections and a 5-point scale described in Experimental Section. ^b Osteoclast counts (Five, 400× fields) were performed on ankles in the areas of greatest bone resorption. ^c Groups (*n* = 8) were dosed with vehicle or **37** orally twice daily beginning on day 8 until sacrifice on day 21. Values represent group means and (SEM). **p* < 0.05 vs vehicle; ***p* < 0.001 vs vehicle (Student's *t* test).

A rat tolerability study was carried out to differentiate compounds **37** and **45**. While **37** was well tolerated at doses of 10 and 40 mg/kg, rats treated with **45** showed nonspecific signs of toxicity such as mucoid feces, cold body, and weight loss (data not shown).

Selectivity profiles of some of these FMS inhibitors against other type III receptor tyrosine kinases were obtained (Table

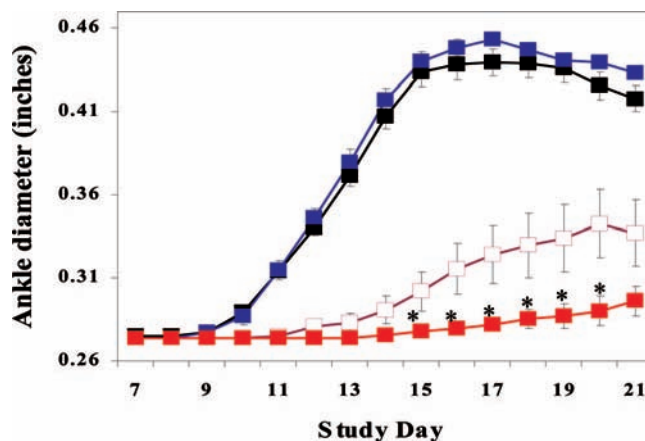


Figure 6. Compound **37** reduced ankle swelling in adjuvant-induced arthritis in combination with methotrexate. Adjuvant arthritis was induced in rats as described in the Experimental Section. Oral dosing was commenced on day 8. Blue squares, dosed twice daily with 20% HPβCD and once daily with 1% carboxymethylcellulose (CMC); black squares, dosed twice daily with 0.33 mg/kg **37** in 20% HPβCD and once daily with 1% CMC; white squares, dosed twice daily with 20% HPβCD and once daily with 0.1 mg/kg methotrexate in 1% CMC; red squares, dosed twice daily with 0.33 mg/kg **37** in 20% HPβCD and once daily with 0.1 mg/kg methotrexate in 1% CMC. Calipers were used to measure ankle thickness daily (mean ± SEM). **p* < 0.05 vs methotrexate alone.

5). In the enzyme assays all were potent inhibitors of FLT3 and KIT but highly selective vs PDGFR-β, Axl, IRK, TrkA,

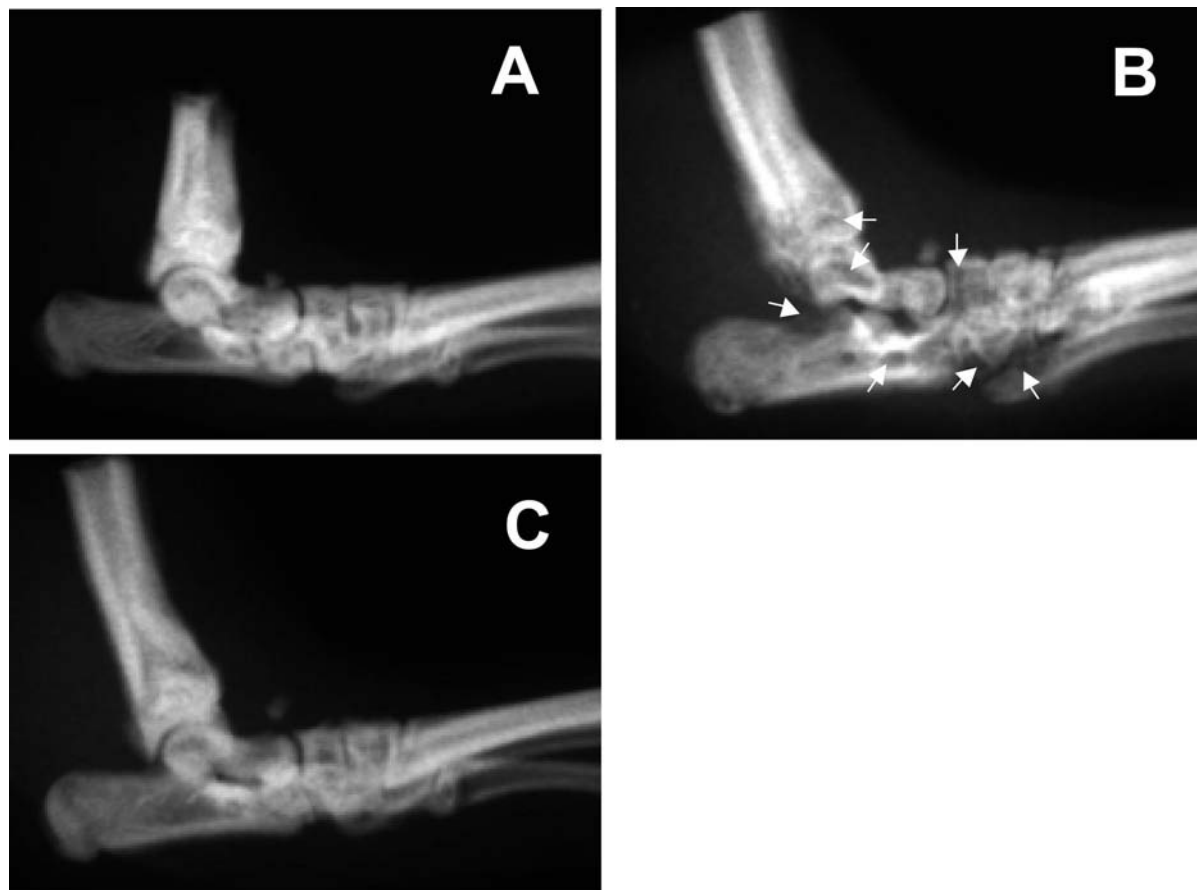


Figure 5. Compound **37** prevented the development of bone lesions in the tibial tarsal joint. Following necropsy on day 21, microradiographic images were prepared of tibial tarsal joints. Representative images are shown obtained from a disease-free rat (A), a rat with adjuvant-arthritis treated with vehicle (B), and a rat with adjuvant-arthritis treated with 1 mg/kg **37** (C). Note the presence of radiotranslucent pits (arrows) in the tibia, calcaneus, talus, and tarsus of the rat with adjuvant-arthritis treated with vehicle, while the tibial tarsal joint of the rat with adjuvant-arthritis treated with **37** was difficult to discern from the disease-free rat.

and Src. In the cell-based assays of these kinases, **37** inhibited ITD-FLT3-dependent MV-4-11 cell growth²³ and SCF/KIT-dependent M-07e cell growth³³ with mean IC₅₀ values of 80 nM and 20 nM, respectively ($n = 4$). Relative to CSF-1/FMS-dependent BMDM cell growth (IC₅₀ = 0.6 nM), this represented modest selectivity versus KIT (33-fold) and good selectivity over FLT3 (133-fold). Inhibition of KIT and FLT3 may have anti-inflammatory potential due to suppression of mast cell or dendritic cell functions, but chronic inhibition of KIT may result in anemia and myelosuppression.³⁴

The pharmacokinetic profiles of **37** in mouse, dog, and monkey were assessed (Table 6). In the mouse, **37** had good bioavailability (51%), an oral C_{max} of 0.9 μ M at a 10 mg/kg dose and a moderate clearance rate. In the dog and monkey, **37** had lower C_{max} levels of 0.12 and 0.06 μ M, respectively. The clearance rates in both species were also high, in line with its low liver microsomal stability (51% and 14% remaining after 10 min incubation in dog and monkey liver microsomes, respectively).

Compound **37** was further evaluated in *in vivo* studies. A pharmacodynamic model was developed based on the ability of CSF-1 to elevate macrophage c-fos mRNA.³⁵ Because significant numbers of macrophages are present in the spleen, spleens of mice were assessed for c-fos mRNA following intravenous administration of 1 μ g/mouse recombinant CSF-1. Splenic c-fos mRNA was increased by approximately 10-fold within 15 min after CSF-1 induction (Figure 2) and returned to baseline by 30 min (data not shown). An oral dose of 3 mg/kg of **37**, administered 6 h prior to the CSF-1 challenge, reduced c-fos mRNA induction by 90% (Figure 2). The corresponding plasma concentration of **37** at the 6 h time point was 0.29 μ M.

Compound **37** was further evaluated in rats using streptococcal cell wall (SCW)-induced and adjuvant-induced models of arthritis. Both models are responsive to prednisone and anti-TNF therapy, and adjuvant arthritis is responsive to methotrexate.³⁶ SCW-induced polyarthritis in female Lewis rats is characterized by an acute, transient phase (days 3–7) that is complement- and neutrophil-dependent, which evolves into a chronic erosive phase (after day 10) that is dependent on the development of specific T cell immunity to SCW.³⁷ An important characteristic of the SCW model is the predominance of macrophages in the inflamed synovial pannus³⁸ that accurately models macrophage involvement in rheumatoid arthritis.³⁹ For this reason, the chronic phase of the SCW-induced arthritis model was selected to investigate the ability of **37** to reduce chronic joint inflammation and bone erosion. Twice-daily oral dosing was initiated on day 19 when chronic inflammation was well established, and **37** was highly effective at reversing established ankle swelling at doses of 10, 3, or 1 mg/kg (Figure 3). The progressive increase in ankle thickness in the vehicle-treated group was delayed in rats dosed with 0.3 mg/kg of **37**.

Compound **37** was less effective in preventing the progressive inflammatory response in adjuvant-induced arthritis. When dosed twice daily from the onset of arthritis (day 8), **37** reduced paw swelling partially at 10 mg/kg, with lower doses showing no improvement (Figure 4 and Table 7). Despite the limited effect on inflammation, microscopic examination revealed preservation of the bones of the tibiotarsal joint. Preservation was nearly complete at 1 mg/kg, and good partial protection was observed even at 0.33 mg/kg (Table 7). By day 21, osteoclasts were abundant in the pannus and trabecular bone of adjuvant rats treated with vehicle. In contrast, there was minimal evidence of reactive osteoclastogenesis in the tibiotarsal joints of rats

dosed with 1 mg/kg of **37**. Microradiographs of representative paws further confirmed the impressive protection of bone structures by **37** (Figure 5). In vehicle-treated rats, foci of increased radiotranslucency were apparent in the distal tibia, while calcaneus, talus, and tarsus bones were frequently difficult to delineate. In contrast, bones from animals treated with **37** (1 mg/kg) were similar to those of disease-free rats. Mean plasma levels taken 7 h after the last dose of 0.33, 1, and 3 mg/kg were 0.014, 0.055, and 0.189 μ M, respectively.

The disease modifying activity of **37** in adjuvant arthritis was further examined in combination with methotrexate, the standard first line therapy for RA. A low dose of **37** (0.33 mg/kg) was administered alone or in combination with an efficacious dose of methotrexate and compared to methotrexate alone. As before, 0.33 mg/kg of **37** alone did not reduce ankle swelling (Figure 6). However, **37** significantly reduced to nearly undetectable levels the mild swelling and inflammation otherwise present in rats administered methotrexate alone. By day 20, swelling was evident in only 2 of 16 ankles in the combination group compared to 12 of 16 joints in the methotrexate alone group.

The anti-inflammatory effects of **37** in the SCW-induced and adjuvant-induced arthritis models are consistent with the requirement for FMS for optimal macrophage survival and proliferation. Indeed, mice that are genetically deficient in FMS or CSF-1 lack synovial macrophages⁴⁰ and CSF-1-deficient mice are highly resistant to collagen-induced arthritis.^{41,42} Similarly, the bone preserving effect of **37** is consistent with the requirement for FMS/CSF-1 for osteoclast differentiation revealed by severe osteopetrosis of the FMS-deficient mice⁴⁰ and the ability of FMS neutralizing antibody to block TNF-induced osteolysis.¹⁵ We therefore attribute the therapeutic effects of **37** primarily to FMS inhibition, although we cannot exclude the possibility that inhibition of secondary targets may contribute to the pharmacology of **37**. Indeed, inhibition of KIT or FLT3 may augment the beneficial pharmacology of **37**, although at the cellular level the selectivity of **37** for FMS was 33- and 133-fold vs KIT and FLT3, respectively. Other FMS inhibitors (i.e., **1**, **2**, and **8**) have demonstrated efficacy in rodent models of arthritis despite nonoverlapping selectivity profiles, further supporting FMS as a promising target for the treatment of rheumatoid arthritis.^{16,17,23b} At present, the primary advantage of **37** may be its exemplary potency.

Conclusion

A novel class of FMS kinase inhibitors based on the pyrido[2,3-*d*]pyrimidin-5-one scaffold was developed. Introduction of a C-6 hydroxamate group resulted in significant potency increases in the cell-based BMDM assay and an improved pharmacokinetic profile. The cocrystal structure of **25** in FMS revealed a complex hydrogen-bonding network between the hydroxamate group and the kinase active site, which is believed to contribute to the improved potency. Further optimization afforded **37**. Among known FMS inhibitors, **37** demonstrated exemplary *in vitro* potency together with outstanding rodent PK. Compound **37** reversed established ankle swelling in the chronic phase of SCW arthritis and enhanced the anti-inflammatory activity of methotrexate in adjuvant arthritis as well as providing profound suppression of bone erosion as a single agent. Collectively, the data provide strong preclinical validation for testing the therapeutic utility of FMS inhibitors in RA, both for

the treatment of signs and symptoms and to prevent the loss of function resulting from joint erosions.

Experimental Section

Chemistry. Reagents and solvents were obtained from commercial suppliers and used without further purification. Flash chromatography was performed using Fisher Chemical Silica Gel Sorbent (230–400 mesh, grade 60). Preparative thin-layer chromatography was performed on Analtech Silica Gel GF plates (1000 or 2000 μ m, 20 cm \times 20 cm). Preparative HPLC was performed on a Gilson 215 HPLC system using a C-18 YMC ODS-A 5m 30 \times 100 mm, 120 Å column with a flow rate of 32 mL/min. The solvents, both acetonitrile (MeCN) and water, contain 0.1% of trifluoroacetic acid (TFA, v/v). Hydrogenation was performed in a H-Cube (ThalesNano, Inc., Budapest, Hungary). ^1H NMR spectra were recorded on a Bruker B-ACS-120 (400 MHz) spectrophotometer at rt. Chemical shifts are given in ppm (δ), coupling constants (J) are in hertz (Hz), and signals are designed as follows: (s) singlet, (d) doublet, (t) triplet, (q) quartet, (m) multiplet, (br s) broad singlet, (dd) doublet of doublet, (dt) doublet of triplet. Elemental analysis was performed by Quantitative Technologies, Inc., Whitehouse, NJ. LC-MS was performed on a system consisting of an atmospheric pressure ionization (API) source on a Finnigan LCQ ion trap mass spectrometer, an Agilent 1100 DAD UV detector (214 nm wavelength), an Agilent 1100-LC binary gradient pumping system, a Gilson 215 configured as an autosampler, and a Zorbax SB-C18 HPLC column (5 μ m, 50 mm \times 2.1 mm). The purities of the key target compounds were determined on the Finnigan LCQ instrument, which gave both the MS and LC trace of the compound in an 11 min run. The HPLC method used was as follows: column, Zorbax SB-C18 HPLC column (5 μ m, 50 mm \times 2.1 mm); column temperature, ambient; flow rate, 0.5 mL/min; gradient, 5% acetonitrile in water to 100% acetonitrile in water in 10 min, both MeCN and water contain 0.1% of TFA, v/v.

3-(Indan-5-ylamino)-propionic Acid Ethyl Ester (11). Tetraabutylammonium bromide (200 mg) was added to a mixture of 5-aminoindan (5 g, 37.6 mmol), ethyl 3-chloropropionate (4.7 mL, 37.6 mmol), and potassium carbonate (5.2 g, 37.6 mmol). The mixture was stirred at 100 °C for 16 h. After cooling to rt, the mixture was extracted into ethyl acetate, washed with water and brine, and dried with sodium sulfate (Na_2SO_4). After evaporation of the solvent and chromatography on silica (eluted with ethyl acetate/hexanes, 1:20 to 1:10, v/v), the title compound was obtained as brown oil (6.2 g, 71%). ^1H NMR (300 MHz, CDCl_3) δ 7.04 (d, J = 7.91 Hz, 1H), 6.56 (s, 1H), 6.45 (dd, J = 1.98, 7.91 Hz, 1H), 4.15 (q, J = 7.09 Hz, 2H), 3.44 (t, J = 6.43 Hz, 2H), 2.82 (q, J = 7.69 Hz, 4H), 2.61 (t, J = 6.43 Hz, 2H), 1.94 – 2.13 (m, 2H), 1.27 (t, J = 7.09 Hz, 3H).

4-[(2-Ethoxycarbonyl)ethyl]-indan-5-yl-amino]-2-methylsulfonylpyrimidine-5-carboxylic Acid Ethyl Ester (12). To a solution of **11** (5 g, 21.4 mmol) and ethyl 4-chloro-2-methylthio-5-pyrimidinecarboxylate (5 g, 21.4 mmol) in 40 mL of *n*-butanol was added triethylamine (3 mL, 21.4 mmol). The solution was stirred at rt for 2 days. The solvent was removed under vacuum. The residue was extracted into EtOAc, washed with water and brine, and dried with Na_2SO_4 . The solvent was removed and the residue was purified by flash chromatography (eluted with ethyl acetate/hexanes, 1:10 to 1:6, v/v) to yield the title compound as a white solid (8.2 g, 90%). ^1H NMR (300 MHz, CDCl_3) δ 8.24 (s, 1H), 7.17 (d, J = 7.91 Hz, 1H), 6.96 (s, 1H), 6.85–6.92 (m, 1H), 4.28–4.39 (m, 2H), 4.05 (q, J = 7.03 Hz, 2H), 3.57 (q, J = 6.92 Hz, 2H), 2.86 (t, J = 7.42 Hz, 4H), 2.63–2.72 (m, 2H), 2.55 (s, 3H), 2.00–2.13 (m, 2H), 1.19 (t, J = 7.25 Hz, 3H), 1.01 (t, J = 7.25 Hz, 3H).

8-Indan-5-yl-2-methylsulfonyl-5-oxo-5,6,7,8-tetrahydropyrido[2,3-*d*]pyrimidine-6-carboxylic Acid Ethyl Ester (13). To sodium (25 wt % dispersion in paraffin wax, 1.6 g, 16.9 mmol) was added *t*-butanol (30 mL) under N_2 with stirring. After 10 min, a solution of **12** (6.6 g, 15.4 mmol) in 40 mL of toluene was added to the sodium *t*-butoxide solution. The mixture was then heated at 90 °C

for 30 min. The solution was cooled and poured into crushed ice. The solution was adjusted to pH 7 using concentrated aq HCl. The precipitates were extracted into ethyl acetate (2 \times 30 mL). The solvent was evaporated under vacuum and the product (bright-yellow solid, 4 g, 62%) was recrystallized from isopropanol. ^1H NMR (300 MHz, CDCl_3) indicated that the presence of both enol and keto forms in a 4:1 ratio.

8-Indan-5-yl-2-methylsulfonyl-5-oxo-5,8-dihydropyrido[2,3-*d*]pyrimidine-6-carboxylic Acid Ethyl Ester (14). To a solution of **13** (0.32 g, 0.84 mmol) in 5 mL of methylene chloride (CH_2Cl_2) was added bromine (43 μ L, 0.84 mmol) slowly under N_2 . The solution was stirred at rt for 2 h. The solvent was removed under vacuum without heating. The residue was dissolved in CH_2Cl_2 (2 mL), to which was added triethylamine (234 μ L, 1.68 mmol) in 1 mL of CH_2Cl_2 . The solution was stirred at rt for 4 h. The solvent was evaporated and the residue was purified by flash chromatography (eluted with ethyl acetate/hexanes, 1:5 to 2:5, v/v). The title compound was obtained as a white solid (0.30 g, 94%). ^1H NMR (300 MHz, CDCl_3) δ 9.42 (s, 1H), 8.59 (s, 1H), 7.37 (d, J = 7.91 Hz, 1H), 7.23–7.25 (m, 1H), 7.16 (d, J = 7.91 Hz, 1H), 4.39 (q, J = 7.14 Hz, 2H), 2.96–3.05 (m, 4H), 2.33 (s, 3H), 2.16–2.25 (m, 2H), 1.40 (t, J = 7.09 Hz, 3H).

8-Indan-5-yl-2-methanesulfonyl-5-oxo-5,8-dihydropyrido[2,3-*d*]pyrimidine-6-carboxylic Acid Ethyl Ester (15). To a solution of **14** (0.3 g, 0.79 mmol) in 5 mL of CH_2Cl_2 , was added 3-chloroperoxybenzoic acid (*m*-CPBA, 69.5%, 431 mg, 1.73 mmol) portionwise. The solution was stirred at rt for 3 h. An aqueous solution of 10% sodium thiosulfate (2 mL) was added to quench the reaction. After 30 min, saturated sodium bicarbonate solution (10 mL) was added, and the aqueous solution was extracted by CH_2Cl_2 (2 \times 10 mL). The combined organic layer was washed with brine and dried over Na_2SO_4 . The solvent was evaporated and the residue was purified by flash chromatography (eluted with ethyl acetate/hexanes, 1:3 to 2:3, v/v). The title compound was obtained as an off-white solid (0.22 g, 67%). ^1H NMR (300 MHz, CDCl_3) δ 9.74 (s, 1H), 8.70 (s, 1H), 7.39 (d, J = 7.91 Hz, 1H), 7.25 (s, 1H), 7.12–7.21 (m, 1H), 4.38 (q, J = 7.25 Hz, 2H), 3.19 (s, 3H), 2.93–3.06 (m, 4H), 2.11–2.27 (m, 2H), 1.38 (t, J = 7.25 Hz, 3H).

8-Indan-5-yl-2-[4-(2-methylpiperazin-1-yl)-ethyl]phenylamino]-5-oxo-5,8-dihydropyrido[2,3-*d*]pyrimidine-6-carboxylic Acid Ethyl Ester (16a). The mixture of 4-[2-(4-methylpiperazin-1-yl)-ethyl]-phenylamine (53 mg, 0.24 mmol) and **15** (100 mg, 0.24 mmol) in 1 mL of isopropanol was heated to 90 °C for 1 h. The solvent was evaporated and the residue was redissolved in a mixture of methanol and CH_2Cl_2 (1:1, v/v) and applied to a preparative TLC plate (2000 micro). The plate was developed in $\text{NH}_4\text{OH}/\text{MeOH}/\text{CH}_2\text{Cl}_2$ (1:9:90, v/v/v). The title compound was obtained as a yellow solid (70 mg, 53%). ^1H NMR (400 MHz, CDCl_3) δ 9.32 (br s, 1H), 8.52 (br s, 1H), 8.18 (br s, 1H), 7.40 (d, J = 7.43 Hz, 1H), 7.23 (br s, 3H), 7.16 (d, J = 7.43 Hz, 1H), 6.90 (br s, 2H), 4.35 (q, J = 7.04 Hz, 2H), 3.05 (t, J = 6.85 Hz, 2H), 2.98 (t, J = 7.24 Hz, 2H), 2.66–2.77 (m, 2H), 2.41–2.64 (m, 8H), 2.37 (br s, 2H), 2.29 (s, 3H), 2.14–2.26 (m, 2H), 1.36 (t, J = 7.04 Hz, 3H).

8-Indan-5-yl-2-[4-(2-morpholin-4-yl-ethyl)phenylamino]-5-oxo-5,8-dihydropyrido[2,3-*d*]pyrimidine-6-carboxylic Acid Ethyl Ester (16b). Using a similar procedure described in the preparation of **16a**, the title compound was prepared from 4-(2-morpholin-4-yl-ethyl)-phenylamine (49 mg, 0.24 mmol) and **15** (100 mg, 0.24 mmol). The title compound was obtained as a yellow solid (60 mg, 46%). ^1H NMR (400 MHz, CDCl_3) δ 9.27 (s, 1H), 8.47 (s, 1H), 8.21 (br s, 1H), 7.35 (d, J = 7.43 Hz, 1H), 7.20 (d, J = 5.09 Hz, 3H), 7.11 (d, J = 7.43 Hz, 1H), 6.85 (br s, 2H), 4.30 (q, J = 7.04 Hz, 2H), 3.68 (br s, 4H), 3.00 (t, J = 6.85 Hz, 2H), 2.93 (t, J = 7.04 Hz, 2H), 2.58–2.72 (m, 2H), 2.36–2.54 (m, 6H), 2.07–2.23 (m, 2H), 1.31 (t, J = 7.04 Hz, 3H).

8-Indan-5-yl-2-[4-(2-(4-methylpiperazin-1-yl)-ethyl)phenylamino]-5-oxo-5,8-dihydropyrido[2,3-*d*]pyrimidine-6-carboxylic Acid Amide (17a). To the solution of **16a** (20 mg, 0.036 mmol) in methanol (2 mL) was bubbled ammonia at -78 °C for 5 min in a pressure bottle.

The bottle was then capped and warmed up to rt with stirring for 16 h. The solvent was evaporated to leave a yellow solid, which was purified by preparative HPLC (MeCN/H₂O, 1:19 to 4:1, v/v, linear gradient over 12 min). The fractions were pooled and made basic with sat. NaHCO₃ solution and were then extracted with CH₂Cl₂. The organic layer was dried over Na₂SO₄ and filtered. The solvent was evaporated to leave a yellow solid, which was treated with 1 N aq HCl solution to give a dihydrochloride salt (5.8 mg, 30%). ¹H NMR (300 MHz, DMSO-*d*₆) δ 10.48 (br s, 1H), 9.31 (s, 1H), 9.10 (s, 1H), 8.62 (s, 1H), 7.75 (m, 1H), 7.54 (m, 2H), 7.41 (m, 2H), 6.97 (br, 2H), 3.55 (m, 4H), 3.09 (t, *J* = 7.31 Hz, 2H), 3.01 (t, *J* = 7.42 Hz, 2H), 2.71 (m, 2H), 2.57 (m, 13H), 2.22 (m, 2H). Anal. (C₃₀H₃₅Cl₂N₇O₂·0.35H₂O) C, H, N, Cl, H₂O.

8-Indan-5-yl-2-[4-[2-(4-methylpiperazin-1-yl)ethyl]phenylamino]-5-oxo-5,8-dihydropyrido[2,3-*d*]pyrimidine-6-carboxylic Acid Methyl Amide (17b). To the solution of **16a** (20 mg, 0.036 mmol) in 1 mL methanol was added a solution of methylamine in THF (2 N, 2 mL). The mixture was stirred at 80 °C for 4 h. The solvent was removed by vacuum to leave a yellow solid. After a preparative HPLC purification (MeCN/H₂O 1:20 to 100:0, v/v, linear gradient over 10 min), a yellow solid was obtained (5.1 mg, 26%). ¹H NMR (400 MHz, CDCl₃/CD₃OD 20:1, v/v) δ 9.61 (m, 1H), 9.29 (s, 1H), 8.75 (s, 1H), 7.35 (d, *J* = 7.83 Hz, 1H), 7.19 (m, 3H), 7.09 (d, *J* = 7.83 Hz, 1H), 6.84 (br s, 2H), 3.00–2.90 (m, 7H), 2.64 (m, 2H), 2.47 (m, 10H), 2.24 (s, 3H), 2.15 (m, 2H). Mass spectrum (LCMS, ESI pos.) calcd for C₃₁H₃₅N₇O₂, 538.29 (M + H); found, 538.2. HPLC: *t*_R = 4.24 min (100% pure).

8-Indan-5-yl-2-[4-(2-morpholin-4-yl-ethyl)phenylamino]-5-oxo-5,8-dihydropyrido[2,3-*d*]pyrimidine-6-carboxylic Acid Methyl Amide (17c). The ester **16b** (20 mg, 0.037 mmol) was converted to the methyl amide **17c** (yellow solid, 17 mg, 87%) using a similar procedure as described in the preparation of **17b**. ¹H NMR (400 MHz, CDCl₃) δ 10.60 (br s, 1H), 9.29 (s, 1H), 8.78 (s, 1H), 7.75 (s, 1H), 7.60 (br s, 1H), 7.34 (d, *J* = 7.83 Hz, 1H), 7.20 (m, 2H), 7.12 (d, *J* = 7.43 Hz, 1H), 6.87 (br s, 2H), 3.69 (t, *J* = 4.30 Hz, 4H), 3.01 (t, *J* = 6.85 Hz, 2H), 2.88–3.06 (m, 5H), 2.61–2.73 (m, 2H), 2.38–2.55 (m, 6H), 2.16 (quin, *J* = 7.24 Hz, 2H). Mass spectrum (LCMS, ESI pos.) calcd for C₃₀H₃₂N₆O₃, 525.25 (M + H); found 525.2. HPLC: *t*_R = 4.66 min (100% pure).

8-Indan-5-yl-2-[4-[2-(4-methylpiperazin-1-yl)ethyl]phenylamino]-5-oxo-5,8-dihydropyrido[2,3-*d*]pyrimidine-6-carboxylic Acid Ethyl Amide (17d). To the solution of **16a** (20 mg, 0.036 mmol) in 1 mL methanol was added a solution of ethylamine in THF (2 N, 2 mL). The mixture was stirred at 80 °C for 16 h. The solvent was removed by vacuum to leave a yellow solid. After a preparative HPLC purification (MeCN/H₂O 1:20 to 100:0, v/v, linear gradient over 10 min), a yellow solid was obtained (7.1 mg, 36%). ¹H NMR (400 MHz, CDCl₃/CD₃OD 20:1 v/v) δ 9.69 (br s, 1H), 9.37 (s, 1H), 8.84 (br s, 1H), 7.41 (d, *J* = 7.83 Hz, 1H), 7.26 (s, 3H), 7.17 (d, *J* = 7.83 Hz, 1H), 6.85 (br s, 2H), 3.50 (q, *J* = 7.24 Hz, 2H), 3.05 (t, *J* = 7.04 Hz, 2H), 2.98 (t, *J* = 7.04 Hz, 2H), 2.66–2.82 (m, 4H), 2.38–2.64 (m, 8H), 2.31 (s, 3H), 2.12–2.28 (m, 2H), 1.27 (t, *J* = 7.24 Hz, 3H). Mass spectrum (LCMS, ESI pos.) calcd for C₃₂H₃₇N₇O₂, 553.30 (M + H); found 553.3. HPLC: *t*_R = 4.56 min (100% pure).

8-Indan-5-yl-2-[4-[2-(4-methylpiperazin-1-yl)ethyl]phenylamino]-5-oxo-5,8-dihydropyrido[2,3-*d*]pyrimidine-6-carboxylic Acid (2-Hydroxyethyl)amide (17e). To a solution of **16a** (25 mg, 0.045 mmol) in methanol (1 mL) was added 2-aminoethanol (0.5 mL). The sealed vial was heated at 110 °C overnight. The solvent was evaporated under vacuum, and the residue was purified by preparative HPLC (MeCN/H₂O 1:19 to 4:1, v/v, linear gradient over 12 min). The title compound was obtained as an off-white solid (22.8 mg, TFA salt, 64%). ¹H NMR (400 MHz, CDCl₃/CD₃OD 10:1, v/v) δ 9.30 (s, 1H), 8.75 (s, 1H), 7.38 (d, *J* = 7.83 Hz, 1H), 7.22 (m, 3H), 7.15 (d, *J* = 7.83 Hz, 1H), 6.90 (br s, 2H), 3.72 (t, *J* = 5.28 Hz, 2H), 3.55 (t, *J* = 5.28 Hz, 2H), 2.90 (m, 4H), 2.30–2.80 (m, 15H), 2.18 (m, 2H). Mass spectrum (LCMS, ESI pos.) calcd for C₃₂H₃₇N₇O₃, 568.30 (M + H); found, 568.3. HPLC: *t*_R = 4.03 min (100% pure).

8-Indan-5-yl-2-[4-[2-(4-methylpiperazin-1-yl)ethyl]phenylamino]-5-oxo-5,8-dihydropyrido[2,3-*d*]pyrimidine-6-carboxylic Acid Methoxyamide (18a). To a mixture of **16a** (10 mg, 0.018 mmol) and methoxyamine hydrochloride (141 mg) in methanol (0.5 mL) was added triethylamine (1 mL). The sealed vial was stirred at 100 °C for 12 h. After cooling, water (20 mL) was added and the mixture was extracted with CH₂Cl₂ (30 mL). The organic layer was washed with brine and dried over Na₂SO₄. The solvent was evaporated under vacuum and the residue was purified by preparative HPLC (MeCN/H₂O 1:19 to 4:1, v/v linear gradient over 12 min). The fractions were pooled, made basic with sat. NaHCO₃ solution, and were then extracted with CH₂Cl₂. The organic layer was dried over Na₂SO₄ and filtered. The solvent was evaporated to leave a yellow solid, which was treated with 1 N HCl solution to give a dihydrochloride salt (yellow solid, 8.6 mg, 86%). ¹H NMR (400 MHz, CDCl₃) δ 11.98 (s, 1H), 9.32 (d, *J* = 4.30 Hz, 1H), 8.83 (br s, 1H), 8.01 (br s, 1H), 7.40 (d, *J* = 7.43 Hz, 1H), 7.24 (br s, 3H), 7.14 (d, *J* = 6.65 Hz, 1H), 6.90 (br s, 2H), 3.88 (s, 3H), 3.05 (t, *J* = 6.85 Hz, 2H), 2.97 (t, *J* = 7.43 Hz, 3H), 2.66–2.78 (m, 2H), 2.41–2.65 (m, 10H), 2.31 (s, 3H), 2.21 (quin, *J* = 7.34 Hz, 2H). Mass spectrum (LCMS, ESI pos.) calcd for C₃₁H₃₅N₇O₃, 554.28 (M + H); found, 554.2. Anal. (C₃₁H₃₇Cl₂N₇O₃·3H₂O) C, H, N, Cl.

8-Indan-5-yl-2-[4-[2-(4-methylpiperazin-1-yl)ethyl]phenylamino]-5-oxo-5,8-dihydropyrido[2,3-*d*]pyrimidine-6-carboxylic Acid Ethoxyamide (18b). Using a similar procedure described in the preparation of **18a**, the title compound was prepared from ethoxyamine hydrochloride (150 mg) and **16a** (10 mg, 0.018 mmol). The title compound was obtained as a yellow solid (6 mg, 60%). ¹H NMR (400 MHz, CDCl₃) δ 11.83 (s, 1H), 9.30 (s, 1H), 8.78 (s, 1H), 7.58 (br s, 1H), 7.36 (d, *J* = 7.43 Hz, 1H), 7.20 (br s, 3H), 7.10 (d, *J* = 7.43 Hz, 1H), 6.85 (br s, 2H), 4.03 (q, *J* = 7.04 Hz, 2H), 3.05 (t, *J* = 6.85 Hz, 2H), 2.95 (t, *J* = 7.42 Hz, 2H), 2.50–2.80 (m, 12H), 2.38 (s, 3H), 2.20 (m, 2H), 1.30 (t, *J* = 7.04 Hz, 3H). Mass spectrum (LCMS, ESI pos.) calcd for C₃₂H₃₇N₇O₃, 568.30 (M + H); found 568.3. HPLC: *t*_R = 4.41 min (100% pure).

8-Indan-5-yl-2-[4-[2-(4-methylpiperazin-1-yl)ethyl]phenylamino]-5-oxo-5,8-dihydropyrido[2,3-*d*]pyrimidine-6-carboxylic Acid Isopropoxyamide (18c). Using a similar procedure described in the preparation of **18a**, the title compound was prepared from *O*-isopropylhydroxylamine hydrochloride (170 mg) and **16a** (10 mg, 0.018 mmol). The title compound was obtained as a yellow solid (4.8 mg, 46%). ¹H NMR (400 MHz, CDCl₃) δ 11.83 (s, 1H), 9.35 (br s, 1H), 8.82 (br s, 1H), 7.70 (br s, 1H), 7.41 (d, *J* = 8.22 Hz, 1H), 7.26 (br s, 3H), 7.16 (d, *J* = 7.83 Hz, 1H), 6.91 (br s, 2H), 4.28 (dt, *J* = 6.21, 12.23 Hz, 1H), 3.06 (t, *J* = 7.24 Hz, 2H), 2.99 (t, *J* = 7.24 Hz, 2H), 2.69–2.80 (m, 2H), 2.40–2.68 (m, 10H), 2.33 (s, 3H), 2.22 (quin, *J* = 7.43 Hz, 2H), 1.35 (s, 3H), 1.33 (s, 3H). Mass spectrum (LCMS, ESI pos.) calcd for C₃₃H₃₉N₇O₃, 582.31 (M + H); found, 582.2. HPLC: *t*_R = 4.66 min (100% pure).

4-Methoxy-2-methylsulfanylpurimidine-5-carboxylic Acid (19). To a suspension of ethyl 4-chloro-2-methylthio-5-pyrimidinecarboxylate (20 g, 86 mmol) in 100 mL of MeOH was added 200 mL of 1 N NaOH solution. After stirring at rt for 3 h, the mixture became a homogeneous orange solution. Ethyl acetate (100 mL) was used to extract the solution and the aqueous solution was acidified with conc aq HCl. The precipitates were twice extracted by ethyl acetate (200 mL). The organic layer was dried over Na₂SO₄ and the solvent was evaporated under vacuum to leave a white solid (16 g, 93%), which was dried under vacuum overnight. ¹H NMR (400 MHz, CDCl₃/CD₃OD 10:1, v/v) δ 8.95 (s, 1H), 4.30 (s, 3H), 2.77 (s, 3H).

3-(4-Methoxy-2-methylsulfanylpurimidin-5-yl)-3-oxo-propionic Acid Ethyl Ester (20). Acid **19** (16 g, 80 mmol) was suspended in CH₂Cl₂ (300 mL) and cooled in an ice bath. To the stirring solution was added a drop of DMF and then oxalyl chloride (23 mL, 258 mmol) dropwise. Upon the completion of the addition, the mixture was allowed to stir at rt for 4 h. The solvent was evaporated without heating to leave a brown solid, which was used for next step without further purification.

To a solution of ethyl hydrogen malonate (23 mL, 214 mmol) in THF (150 mL) was added dropwise MeMgBr in Et₂O (3 M,

143 mL, 429 mmol) under nitrogen in an ice bath. After the mixture was stirred for 20 min, a suspension of the above acid chloride in THF (300 mL) was added slowly. After being stirred at rt for 2 h, the reaction mixture was poured into ice water, acidified to pH 5–6 with conc aq HCl, and twice extracted with ethyl acetate (200 mL). The organic layer was dried over Na₂SO₄ and concentrated under vacuum to afford a crude product, which was purified by flash chromatography (eluted with ethyl acetate/hexanes 1:19 to 1:9, v/v) to give a white solid (7.0 g, 28%). ¹H NMR (400 MHz, CDCl₃) indicated that the presence of both enol and keto forms in a 1:2 ratio: δ 12.64 (s, 1H), 8.85 (s, 2H), 8.84 (s, 1H), 6.03 (s, 1H), 4.25 (q, *J* = 7.17 Hz, 2H), 4.19 (q, *J* = 7.17 Hz, 4H), 4.09 (s, 3H), 4.07(s, 6H), 3.91 (s, 4H), 2.60 (s, 6H), 2.59 (s, 3H), 1.33 (t, *J* = 7.04 Hz, 3H), 1.25 (t, *J* = 7.04 Hz, 6H).

8-Indan-2-methylsulfanyl-5-oxo-5,8-dihydropyrido[2,3-*d*]pyrimidine-6-carboxylic Acid Ethyl Ester (21). A mixture of **20** (10 g, 37 mmol), acetic anhydride (10 mL, 100 mmol), and triethylorthoformate (10 mL, 60 mmol) was heated to reflux at 130 °C for 4 h, during which period the resulting ethyl acetate was distilled off under atmospheric pressure. After concentration under vacuum, the dark-brown oil that was obtained was diluted with THF (100 mL) and 5-aminoindan (5.5 g 39 mmol) was added. The mixture was stirred at rt for 16 h. Then K₂CO₃ (5.6 g, 40 mmol) was added. The mixture was stirred at rt for 16 h. After an aqueous work up using CH₂Cl₂ as extracting solvent, the organic solvent was evaporated to leave a yellow solid, which was used in the next step without further purification.

8-Indan-2-methylsulfanyl-5-oxo-5,8-dihydropyrido[2,3-*d*]pyrimidine-6-carboxylic Acid (22). To a solution of **21** in 1,4-dioxane (100 mL) was added aq HCl (1 N, 120 mL). The mixture was heated to reflux for 4 h. The solution was cooled in an ice water bath, filtered, and the resulting solid was washed with water. The title compound (11.1 g, 85%) was obtained as a white solid after drying under vacuum. ¹H NMR (400 MHz, CDCl₃) δ 14.02 (br s, 1H), 9.50 (br s, 1H), 8.89 (s, 1H), 7.38 (d, *J* = 7.69 Hz, 1H), 7.24 (s, 1H), 7.16 (d, *J* = 7.69 Hz, 1H), 3.01 (q, *J* = 8.12 Hz, 4H), 2.34 (s, 3H), 2.15–2.25 (m, 2H).

8-Indan-5-yl-2-methylsulfanyl-5-oxo-5,8-dihydropyrido[2,3-*d*]pyrimidine-6-carboxylic Acid Methoxyamide (23). To a suspension of **22** (1.30 g, 3.68 mmol) in CH₂Cl₂ (30 mL) at 0 °C was added a drop of DMF followed by oxalyl chloride (0.5 mL, 5.52 mmol). The solution was stirred at rt for 1 h. The solvent was evaporated under vacuum without heating, and the residue was dissolved in CH₂Cl₂ (30 mL). To this solution was added methoxyamine hydrochloride (0.52 g, 6 mmol), followed by slow addition of triethylamine (1.4 mL, 10 mmol) at 0 °C. The solution was stirred at 0 °C for 10 min and rt for 1 h. Water was added and the aqueous solution was twice extracted with CH₂Cl₂ (200 mL). The combined organic layers were dried over Na₂SO₄ and concentrated under vacuum to afford a crude product, which was purified by recrystallization from ethyl acetate/hexanes (2:1, v/v). The title compound was obtained as an off-white solid (1.35 g, 96%). ¹H NMR (400 MHz, CDCl₃) δ 11.84 (s, 1H), 9.45 (br s, 1H), 8.88 (s, 1H), 7.36 (d, *J* = 7.83 Hz, 1H), 7.23 (s, 1H), 7.12–7.17 (m, 1H), 3.90 (s, 3H), 3.00 (q, *J* = 7.69 Hz, 4H), 2.33 (s, 3H), 2.19 (quin, *J* = 7.43 Hz, 2H).

8-Indan-5-yl-2-methanesulfonyl-5-oxo-5,8-dihydropyrido[2,3-*d*]pyrimidine-6-carboxylic Acid Methoxyamide (24). To a stirring solution of **23** (2.4 g, 6.3 mmol) in CH₂Cl₂ (100 mL) was slowly added *m*CPBA (3.8 g, 15.8 mmol) at 0 °C. The mixture was then stirred at rt for 5 h. A Na₂S₂O₃ solution (10%, 20 mL) was added to quench the reaction. The mixture was extracted with CH₂Cl₂ and the organic layer was twice washed with sat. NaHCO₃ solution and dried over Na₂SO₄. The solvent was evaporated to leave a pale-yellow solid (2.3 g, 88%). ¹H NMR (400 MHz, CDCl₃) δ 11.61 (s, 1H), 9.85 (s, 1H), 9.05 (s, 1H), 7.39 (d, *J* = 7.83 Hz, 1H), 7.23 (s, 1H), 7.15 (d, *J* = 8.22 Hz, 1H), 3.91 (s, 3H), 3.22 (s, 3H), 3.01 (q, *J* = 7.43 Hz, 4H), 2.20 (t, *J* = 7.63 Hz, 2H).

8-Cyclohexyl-5-oxo-2-[4-(2-pyrrolidin-1-yl-ethyl)phenylamino]-5,8-dihydropyrido[2,3-*d*]pyrimidine-6-carboxylic Acid Methoxyamide (25). 8-Cyclohexyl-2-methanesulfonyl-5-oxo-5,8-dihydropyrido[2,3-*d*]pyrimidine-6-carboxylic acid ethyl ester (100 mg, 0.26 mmol,

prepared similarly to **15**) and 4-(2-pyrrolidin-1-yl-ethyl)phenylamine (100 mg, 0.53 mmol) in AcOH (1 mL) was heated at 110 °C for 10 min. The reaction mixture was concentrated, and the remaining residue was partitioned between sat. NaHCO₃ and CH₂Cl₂. The organic layer was dried over Na₂SO₄, filtered, and the solvent was evaporated. The residue was purified by preparative HPLC (MeCN/H₂O 1:10 to 10:1, v/v, linear gradient over 12 min). The ester obtained was converted to the title compound using a similar procedure described in the preparation of **18a**. A yellow solid was obtained (50 mg, 39%). ¹H NMR (400 MHz, CDCl₃) δ 11.95 (s, 1H), 9.30 (s, 1H), 8.75 (s, 1H), 7.75 (br s, 1H), 7.55 (d, *J* = 8.61 Hz, 2H), 7.20 (d, *J* = 8.61 Hz, 2H), 5.08 (t, *J* = 11.93 Hz, 1H), 3.81 (s, 3H), 2.79–2.92 (m, 2H), 2.68–2.78 (m, 2H), 2.60 (br, 4H), 1.86–2.10 (m, 6H), 1.56–1.86 (m, 4H), 1.38–1.56 (m, 2H), 1.15–1.38 (m, 2H). Mass spectrum (LCMS, ESI pos.) calcd for C₂₇H₃₄N₆O₃, 491.27 (M + H); found, 491.2. HPLC: *t*_R = 4.39 min (100% pure).

2-Benzylamino-8-indan-5-yl-5-oxo-5,8-dihydropyrido[2,3-*d*]pyrimidine-6-carboxylic Acid Methoxyamide (26). A solution of **24** (30 mg, 0.075 mmol) and benzylamine (16 mg, 0.15 mmol) in acetic acid (1 mL) was stirred at 110 °C for 10 min. A precipitate formed upon cooling, which was filtered and washed with acetonitrile. The white solid (8 mg, 24%) was dried and no further purification was required. ¹H NMR (400 MHz, CDCl₃) δ 12.00 (s, 1H), 9.25 (s, 1H), 8.74 (s, 1H), 7.29–7.35 (m, 2H), 7.22–7.25 (m, 2H), 7.18 (s, 1H), 7.01–7.10 (m, 2H), 6.25 (br s, 1H), 4.34 (d, *J* = 6.26 Hz, 2H), 3.89 (s, 3H), 2.93–3.03 (m, 4H), 2.13–2.22 (m, 2H). Mass spectrum (LCMS, ESI pos.) calcd for C₂₅H₂₃N₅O₃, 442.18 (M + H); found, 442.1. HPLC: *t*_R = 6.74 min (100% pure).

2-Butylamino-8-indan-5-yl-5-oxo-5,8-dihydropyrido[2,3-*d*]pyrimidine-6-carboxylic Acid Methoxyamide (27). A solution of **24** (50 mg, 0.12 mmol) and *n*-butylamine (18 mg, 0.24 mmol) in acetic acid (1 mL) was stirred at 110 °C for 10 min. A precipitate formed upon cooling, which was filtered and washed with acetonitrile. The white solid (15 mg, 30%) was dried and no further purification was required. ¹H NMR (400 MHz, CDCl₃) δ 11.87 (s, 1H), 9.18 (s, 1H), 8.76 (s, 1H), 7.34 (d, *J* = 7.83 Hz, 1H), 7.21 (s, 1H), 7.12 (d, *J* = 7.83 Hz, 1H), 3.89 (s, 3H), 3.12–3.22 (m, 2H), 2.99 (q, *J* = 7.83 Hz, 4H), 2.18 (t, *J* = 7.43 Hz, 2H), 1.44 (t, *J* = 7.24 Hz, 2H), 1.22 (dt, *J* = 7.48, 15.16 Hz, 2H), 0.80 (t, *J* = 7.43 Hz, 3H). Mass spectrum (LCMS, ESI pos.) calcd for C₂₂H₂₅N₅O₃, 408.20 (M + H); found, 408.1. HPLC: *t*_R = 6.91 min (100% pure).

8-Indan-5-yl-2-(6-methoxypyridin-3-ylamino)-5-oxo-5,8-dihydropyrido[2,3-*d*]pyrimidine-6-carboxylic Acid Methoxyamide (28). A solution of **24** (50 mg, 0.12 mmol) and 6-methoxy-pyridin-3-ylamine (50 mg, 0.4 mmol) in acetic acid (1 mL) was stirred at 110 °C for 10 min. The solvent was evaporated, and the residue was purified by preparative HPLC (MeCN/H₂O 1:4 to 100:0, v/v, linear gradient over 12 min). The title compound was obtained as a yellow solid (37.2 mg, 68%). ¹H NMR (400 MHz, CDCl₃/CD₃OD 19:1, v/v) δ 9.34 (s, 1H), 8.81 (br s, 1H), 8.03 (br s, 1H), 7.70 (d, *J* = 7.83 Hz, 1H), 7.41 (d, *J* = 7.83 Hz, 1H), 7.25 (s, 1H), 7.13 (d, *J* = 7.43 Hz, 1H), 6.38 (d, *J* = 8.61 Hz, 1H), 3.90 (s, 3H), 2.95–3.12 (m, 4H), 2.57 (br s, 3H), 2.23 (quin, *J* = 7.43 Hz, 2H). Mass spectrum (LCMS, APCI pos.) calcd for C₂₄H₂₂N₆O₄, 459.17 (M + H); found, 459.1. HPLC: *t*_R = 6.17 min (100% pure).

8-Indan-5-yl-2-[4-(2-morpholin-4-yl-ethyl)phenylamino]-5-oxo-5,8-dihydropyrido[2,3-*d*]pyrimidine-6-carboxylic Acid Methoxyamide (29). A solution of **24** (20 mg, 0.048 mmol) and 4-(2-morpholin-4-yl-ethyl)-phenylamine (18 mg, 0.087 mmol) in acetic acid (1 mL) was stirred at 110 °C for 10 min. The solvent was evaporated, and the residue was purified by preparative HPLC (MeCN/H₂O 1:19 to 4:1, v/v, linear gradient over 12 min). The title compound was obtained as a yellow solid (8 mg, HCl salt, 31%). ¹H NMR (400 MHz, CDCl₃/CD₃OD 10:1 v/v) δ 9.30 (br s, 1H), 8.75 (br s, 1H), 7.40 (d, *J* = 7.43 Hz, 1H), 7.25–7.36 (m, 2H), 7.21 (s, 1H), 7.13 (d, *J* = 7.83 Hz, 1H), 6.93 (br s, 2H), 4.08–4.25 (m, 2H), 3.96 (d, *J* = 10.96 Hz, 2H), 3.84 (s, 3H), 3.47 (d, *J* = 12.13 Hz, 2H), 2.80–3.09 (m, 10H), 2.13–2.32 (m, 2H). Mass spectrum (LCMS, APCI pos.) calcd for C₃₀H₃₂N₆O₄, 541.24 (M + H); found, 541.2. HPLC: *t*_R = 4.61 min (100% pure).

2-[4-[2-(4,4-Difluoropiperidin-1-yl)ethyl]phenylamino]-8-indan-5-yl-5-oxo-5,8-dihydropyrido[2,3-d]pyrimidine-6-carboxylic Acid Methoxyamide (30). A. **4,4-Difluoro-1-[2-(4-nitro-phenyl)-ethyl]-piperidine.** To the solution of the 1-(2-bromo-ethyl)-4-nitro-benzene (450 mg) and 4,4-difluoro-piperidine or 3,3-difluoro-piperidine (250 mg) in DMSO (5 mL) was added K_2CO_3 (400 mg). The mixture was heated at 90 °C for 2 h. Water was added, and the mixture was extracted with CH_2Cl_2 . The combined organic extracts were washed with brine, dried (Na_2SO_4), filtered, and the filtrate concentrated and purified by flash chromatography (EtOAc/hexanes 1:5 v/v) to afford a yellow solid (200 mg). 1H NMR (400 MHz, $CDCl_3$) δ 8.14 (m, 2H), 7.37 (t, 2H, $J = 7.0$), 2.91 (m, 2H), 2.68 (m, 2H), 2.62 (m, 4H), 2.00 (m, 4H).

B. 4-[2-(4,4-Difluoro-piperidin-1-yl)-ethyl]-phenylamine. 4,4-Difluoro-1-[2-(4-nitro-phenyl)-ethyl]-piperidine (200 mg) was dissolved in EtOH/AcOH (6 mL, 1:1 v/v). Iron powder (200 mg) was then added. The mixture was refluxed at 100 °C for 2 h. After cooling down, the mixture was filtered through celite and washed with methanol. The solvent was evaporated, and the residue was suspended in sat. $NaHCO_3$ solution (100 mL). The suspension was extracted with CH_2Cl_2 (100 mL) twice. The organic layers were combined and washed with brine and dried (Na_2SO_4). The solvent was evaporated to leave brown oil, which was used for next step without further purification.

C. 2-[4-[2-(4,4-Difluoropiperidin-1-yl)ethyl]phenylamino]-8-indan-5-yl-5-oxo-5,8-dihydropyrido[2,3-d]pyrimidine-6-carboxylic Acid Methoxyamide (30). A solution of **24** (100 mg, 0.24 mmol) and 4-[2-(4,4-difluoropiperidin-1-yl)ethyl]phenylamine (prepared similarly as **31**, 125 mg, 0.52 mmol) in acetic acid (1 mL) was stirred at 110 °C for 10 min. The solvent was evaporated, and the residue was purified by preparative HPLC (MeCN/ H_2O 1:4 to 100:0, v/v, linear gradient over 12 min). The title compound was obtained as a yellow solid (75.4 mg, 55%). 1H NMR (400 MHz, $CDCl_3$) δ 11.96 (s, 1H), 9.37 (s, 1H), 8.83 (s, 1H), 7.42 (d, $J = 7.83$ Hz, 1H), 7.26 (s, 7H), 7.18 (d, $J = 7.83$ Hz, 1H), 6.93 (br s, 2H), 3.90 (s, 3H), 3.07 (t, $J = 7.33$ Hz, 2H), 3.01 (t, $J = 7.33$ Hz, 2H), 2.69–2.79 (m, 2H), 2.55–2.67 (m, 6H), 2.19–2.29 (m, 2H), 1.95–2.10 (m, 4H). Mass spectrum (LCMS, ESI pos.) calcd for $C_{31}H_{32}F_2N_6O_3$, 575.25 (M + H); found, 575.2. HPLC: $t_R = 5.02$ min (100% pure).

8-Indan-5-yl-5-oxo-2-[4-[2-(3-oxo-piperazin-1-yl)ethyl]phenylamino]-5,8-dihydropyrido[2,3-d]pyrimidine-6-carboxylic Acid Methoxyamide (31). To a solution of 1-(2-bromo-ethyl)-4-nitro-benzene (0.6 g, 2.6 mmol) and 2-piperidinone (0.26 g, 2.6 mmol) in DMSO (10 mL) was added K_2CO_3 (0.4 g, 3.0 mmol). The mixture was stirred at 80 °C for 4 h. Water was then added, and the mixture was twice extracted with CH_2Cl_2 (100 mL). The combined organic extracts were washed with brine, dried over Na_2SO_4 , filtered, and the filtrate concentrated and purified by flash chromatography (ethyl acetate/hexanes 1:5, v/v) to afford an off-white solid. The nitro compound was then reduced to the aniline using H-cube (1 mL/min, 10% Pd/C). 4-[2-(4-Aminophenyl)ethyl]piperazin-2-one was obtained as a yellow solid (0.42 g, 74%). 1H NMR (400 MHz, $CDCl_3$) δ 6.97 (d, $J = 8.22$ Hz, 2H), 6.62 (d, $J = 8.22$ Hz, 2H), 3.51 (br s, 2H), 3.30–3.38 (m, 2H), 3.18 (s, 2H), 2.64–2.72 (m, 4H), 2.55–2.64 (m, 2H).

Using a similar procedure as described in the preparation of **29**, the title compound was prepared from **24** (25 mg, 0.06 mmol) and 4-[2-(4-aminophenyl)ethyl]piperazin-2-one (20 mg, 0.09 mmol). A yellow solid (10.9 mg, HCl salt, 31%) was obtained. 1H NMR (400 MHz, $CDCl_3/CD_3OD$ 19:1, v/v) δ 9.35 (br s, 1H), 8.81 (br s, 1H), 7.44 (d, $J = 7.83$ Hz, 1H), 7.28 (br s, 3H), 7.18 (d, $J = 7.83$ Hz, 1H), 6.91 (br s, 2H), 3.90 (s, 3H), 3.34–3.42 (m, 2H), 3.21 (s, 2H), 3.08 (t, $J = 7.24$ Hz, 2H), 3.01 (t, $J = 7.43$ Hz, 2H), 2.59–2.78 (m, 6H), 2.24 (quin, $J = 7.43$ Hz, 2H). Mass spectrum (LCMS, APCI pos.) calcd for $C_{30}H_{31}N_7O_4$, 554.24 (M + H); found, 554.2. HPLC: $t_R = 4.35$ min (98.8% pure).

8-Indan-5-yl-2-[4-[2-(4-methyl-3-oxo-piperazin-1-yl)ethyl]phenylamino]-5-oxo-5,8-dihydropyrido[2,3-d]pyrimidine-6-carboxylic Acid Methoxyamide (32). Using a similar procedure as described in the preparation of **31**, the title compound was prepared from **24**

(80 mg, 0.19 mmol) and 4-[2-(4-aminophenyl)ethyl]-1-methylpiperazin-2-one (60 mg, 0.26 mmol). The title compound was obtained as a yellow solid (41.1 mg, 38%). 1H NMR (400 MHz, $CDCl_3$) δ 11.97 (s, 1H), 9.36 (br s, 1H), 8.83 (s, 1H), 7.77 (br s, 1H), 7.42 (d, $J = 7.83$ Hz, 1H), 7.27 (s, 3H), 7.10–7.20 (m, 1H), 6.92 (br s, 2H), 3.90 (s, 3H), 3.34 (t, $J = 5.48$ Hz, 2H), 3.21 (s, 2H), 3.07 (t, $J = 7.24$ Hz, 2H), 2.88–3.04 (m, 5H), 2.74 (t, $J = 5.48$ Hz, 4H), 2.54–2.65 (m, 2H), 2.23 (quin, $J = 7.43$ Hz, 2H). Mass spectrum (LCMS, APCI pos.) calcd for $C_{31}H_{33}N_7O_4$, 568.24 (M + H); found, 568.2. HPLC: $t_R = 4.47$ min (99.2% pure).

2-[4-(2-Acetylsulfamoyl-ethyl)phenylamino]-8-indan-5-yl-5-oxo-5,8-dihydropyrido[2,3-d]pyrimidine-6-carboxylic Acid Methoxyamide (33). A. **2-(4-Nitro-phenyl)ethanesulfonyl Chloride.** 1-(2-Bromo-ethyl)-4-nitrobenzene (3 g, 13 mmol) and potassium thioacetate (3 g, 26 mmol) in DMSO (10 mL) were stirred at rt for 3 h. EtOAc was used to dilute the reaction mixture. The organic layer was washed with water twice (2 \times 100 mL) and then with brine and dried over Na_2SO_4 . The solvent was evaporated in vacuo to give a brown solid (~3 g), which was taken up in 50 mL of acetic acid. To the stirring solution was added 20 mL of hydrogen peroxide (30% in water). The resulting yellow solution was stirred at rt overnight. Water (50 mL) was added, and the solvent was evaporated in vacuo with minimal heating. The yellow residue was dried in vacuo for two days, suspended in thionyl chloride (18 mL), and heated at reflux (80 °C) for 6 h. The volatiles were evaporated to give the title compound as a yellow solid, which was used in the next step without further purification.

B. 2-(4-Aminophenyl)ethanesulfonic Acid Acetamide. A mixture of 2-(4-nitro-phenyl)ethanesulfonyl chloride (200 mg, 0.8 mmol) and ammonium hydroxide (5 mL) in CH_2Cl_2 (10 mL) was stirred at rt for 2 h. To the reaction mixture was added CH_2Cl_2 (100 mL) and water (100 mL). The organic fraction was dried over Na_2SO_4 , filtered, and the filtrate was concentrated in vacuo. To a solution of the residue in CH_2Cl_2 (10 mL) was added pyridine (0.3 mL) and acetic anhydride (75 μ L), and the reaction mixture was stirred at rt for 3 days. After an aqueous workup, the reaction mixture was extracted with CH_2Cl_2 . The combined organic fractions were dried over Na_2SO_4 , filtered, and the filtrate was concentrated. The residue was purified by flash chromatography (CH_2Cl_2/CH_3OH 19:1, v/v). The resulting nitro compound was hydrogenated over Pd/C (10%) in methanol under atmospheric pressure. The reaction mixture was filtered, and the filtrate was concentrated to give the title compound as a pink solid (66 mg).

C. 2-[4-(2-Acetylsulfamoyl-ethyl)phenylamino]-8-indan-5-yl-5-oxo-5,8-dihydropyrido[2,3-d]pyrimidine-6-carboxylic Acid Methoxyamide (33). The title compound was prepared by reacting 2-(4-aminophenyl)ethanesulfonic acid acetamide (15 mg, 0.062 mmol) with **24** (20 mg, 0.048 mmol) using a similar procedure as described in the preparation of **31**. 1H NMR (400 MHz, $CDCl_3/CD_3OD$ 10:1 v/v) δ 9.32 (s, 1H), 8.77 (s, 1H), 7.40 (d, $J = 7.81$ Hz, 1H), 7.30 (br, 2H), 7.25 (s, 1H), 7.15 (d, $J = 8.22$ Hz, 1H), 6.90 (br, 2H), 3.85 (s, 3H), 3.58 (m, 2H), 3.00 (m, 6H), 2.20 (m, 2H), 1.95 (s, 3H). Mass spectrum (LCMS, APCI pos.) calcd for $C_{28}H_{28}N_6O_6S$, 577.18 (M + H); found 577.1. HPLC: $t_R = 5.63$ min (100% pure).

8-Indan-5-yl-5-oxo-2-(4-piperidin-4-yl-phenylamino)-5,8-dihydropyrido[2,3-d]pyrimidine-6-carboxylic Acid Methoxyamide (34). The title compound was prepared from **24** (100 mg, 0.24 mmol) and 4-(4-amino-phenyl)-piperidine-1-carboxylic acid *tert*-butyl ester (60 mg, 0.22 mmol) using a similar procedure to that described in the preparation of **29**. The Boc group was removed by TFA. The title compound was obtained as a yellow solid (66 mg, 59%). 1H NMR (400 MHz, $CDCl_3$) δ 11.90 (br s, 1H), 9.30 (br s, 1H), 8.76 (br s, 1H), 7.54 (br s, 1H), 7.36 (d, $J = 7.83$ Hz, 1H), 7.15–7.27 (m, 3H), 7.11 (d, $J = 8.22$ Hz, 1H), 6.88 (br s, 2H), 3.83 (s, 3H), 3.19 (d, $J = 12.13$ Hz, 2H), 3.02 (t, $J = 6.65$ Hz, 2H), 2.94 (t, $J = 7.43$ Hz, 2H), 2.63–2.76 (m, 2H), 2.49 (br s, 1H), 2.17 (quin, $J = 7.24$ Hz, 2H), 1.67–1.79 (m, 2H), 1.62 (br s, 2H). Mass spectrum (LCMS, APCI pos.) calcd for $C_{29}H_{30}N_6O_3$, 511.24 (M + H); found, 511.2. HPLC: $t_R = 4.57$ min (100% pure).

2-[4-[1-(2-Hydroxy-ethyl)piperidin-4-yl]phenylamino]-8-indan-5-yl-5-oxo-5,8-dihydropyrido[2,3-d]pyrimidine-6-carboxylic Acid Methoxyamide (35). To a solution of **34** (36 mg, 0.07 mmol) in DMSO (0.5 mL) was added 2-bromoethanol (7 μ L, 0.1 mmol) and triethylamine (14 μ L, 0.1 mmol). The solution was stirred at 80 °C for 2 h. Water was added, and the mixture was extracted with CH_2Cl_2 (100 mL). The organic layer was dried over Na_2SO_4 , and the solvent was evaporated. The product was purified by preparative HPLC (MeCN/ H_2O 1:19 to 4:1, v/v, linear gradient over 12 min). A yellow solid was obtained (11 mg, 28%). ^1H NMR (400 MHz, CDCl_3) δ 11.98 (s, 1H), 9.36 (br s, 1H), 8.83 (br s, 1H), 7.64 (br s, 1H), 7.43 (d, J = 7.83 Hz, 1H), 7.26 (s, 4H), 7.17 (d, J = 7.83 Hz, 1H), 6.94 (br s, 1H), 3.90 (s, 3H), 3.67 (t, J = 5.28 Hz, 2H), 3.08 (m, 2H), 3.00 (t, J = 7.43 Hz, 2H), 2.57–2.66 (m, 2H), 2.47 (t, J = 11.54 Hz, 1H), 2.16–2.30 (m, 4H), 1.67–1.90 (m, 6H). Mass spectrum (LCMS, ESI pos.) calcd for $\text{C}_{31}\text{H}_{34}\text{N}_6\text{O}_4$, 555.24 (M + H); found, 555.3. HPLC: t_R = 4.48 min (99.6% pure).

[4-[4-(8-Indan-5-yl-6-methoxycarbamoyl-5-oxo-5,8-dihydropyrido[2,3-d]pyrimidin-2-ylamino)phenyl]piperidin-1-yl]-acetic Acid (36). To a solution of **34** (30 mg, 0.06 mmol) in DMSO (2 mL) was added *t*-butyl bromoacetate (10 μ L, 0.065 mmol) and K_2CO_3 (11 mg, 0.08 mmol). The solution was stirred at 60 °C for 1 h. Water was added, and the mixture was extracted with CH_2Cl_2 (100 mL). The organic layer was dried over Na_2SO_4 , and the solvent was evaporated. The solvent was removed under vacuum. The residue was purified by preparative TLC (developed in MeOH/ CH_2Cl_2 1:10, v/v) to afford a yellow solid. The solid was then treated with TFA/ CH_2Cl_2 (5 mL, 1:1 v/v) at rt for 1 h. The solvent was evaporated, and the residue was dissolved in CH_2Cl_2 (50 mL). The organic layer was washed with sat. NaHCO_3 and brine and dried over Na_2SO_4 . The solvent was evaporated to leave a yellow solid (10.5 mg, 31%). ^1H NMR (300 MHz, CD_3OD) δ 9.25 (s, 1H), 8.68 (s, 1H), 7.46 (d, J = 7.83 Hz, 1H), 7.36 (br s, 3H), 7.24 (d, J = 7.83 Hz, 1H), 6.95 (br s, 2H), 4.14 (s, 2H), 3.83 (s, 3H), 3.77 (d, J = 12.13 Hz, 2H), 3.19–3.26 (m, 2H), 3.11 (br s, 2H), 3.01 (t, J = 7.24 Hz, 2H), 2.83 (br s, 1H), 2.17–2.31 (m, 2H), 1.93–2.12 (m, 4H). Mass spectrum (LCMS, APCI pos.) calcd for $\text{C}_{31}\text{H}_{32}\text{N}_6\text{O}_5$, 569.24 (M + H); found, 569.1. HPLC: t_R = 4.53 min (98.9% pure).

8-Indan-5-yl-2-[4-(1-methylpiperidin-4-yl)phenylamino]-5-oxo-5,8-dihydropyrido[2,3-d]pyrimidine-6-carboxylic Acid Methoxyamide (37). To a well-ground mixture of **24** (4 g, 9.66 mmol) and 4-(1-methylpiperidin-4-yl)phenylamine (2.5 g, 13.5 mmol) was added 20 mL of AcOH. The mixture was stirred at 110 °C for 20 min. The AcOH was evaporated under high vacuum. The residue was dissolved in CH_2Cl_2 (400 mL), and the solution was washed with sat. NaHCO_3 and brine. The organic layer was dried over Na_2SO_4 , and the solvent was evaporated. The product was purified by flash chromatography, followed by recrystallization from methanol twice. The off-white solid was dissolved in CH_2Cl_2 and methanol and treated with aq HCl (1 N, 1 equiv). The solvent was evaporated in high vacuum to leave a yellow solid (3.8 g, 70%). ^1H NMR (400 MHz, CDCl_3) δ 11.98 (s, 1H), 9.35 (br s, 1H), 8.82 (br s, 1H), 7.70 (br s, 1H), 7.41 (d, J = 8.22 Hz, 1H), 7.26 (br s, 3H), 7.17 (d, J = 7.83 Hz, 1H), 6.95 (br s, 2H), 3.90 (s, 3H), 3.07 (t, J = 7.04 Hz, 2H), 2.90–3.04 (m, 4H), 2.36–2.48 (m, 1H), 2.32 (s, 3H), 2.23 (quin, J = 7.34 Hz, 2H), 1.95–2.12 (m, 2H), 1.63–1.86 (m, 4H). Mass spectrum (LCMS, ESI pos.) calcd for $\text{C}_{30}\text{H}_{32}\text{N}_6\text{O}_3$, 525.25 (M + H); found, 525.2. Anal. ($\text{C}_{30}\text{H}_{33}\text{ClN}_6\text{O}_3 \cdot 0.3\text{H}_2\text{O}$) C, H, N.

2-[4-(3,3-Difluoro-1-methylpiperidin-4-yl)phenylamino]-8-indan-5-yl-5-oxo-5,8-dihydropyrido[2,3-d]pyrimidine-6-carboxylic Acid Methoxyamide (38). **A. [4-(3-Methoxy-pyridin-4-yl)phenyl]carbamic Acid Benzyl Ester (40).** 4-Bromo-3-methoxy-pyridine (400 mg, 2.13 mmol) and 4-Cbz-amino-phenyl boronic acid (576 mg, 2.13 mmol) was dissolved in a mixture of ethanol (4 mL) and toluene (2 mL). To the solution was added 2 M Na_2CO_3 solution (5 mL). The system was purged with N_2 . $\text{Pd}(\text{PPh}_3)_4$ (20 mg) was added under N_2 . The mixture was refluxed at 110 °C for 2 h. After cooling, water was added, and the reaction mixture was twice extracted with ethyl acetate (30 mL). The organic layer was dried

over Na_2SO_4 and concentrated. The residue was purified by flash chromatography (eluted with ethyl acetate/hexanes 2:3, v/v). A white solid was obtained (563 mg, 79%). ^1H NMR (400 MHz, CDCl_3) δ 8.35 (s, 1H), 8.30 (d, J = 4.80 Hz, 1H), 7.53–7.59 (m, J = 8.59 Hz, 2H), 7.45–7.51 (m, J = 8.59 Hz, 2H), 7.33–7.44 (m, 5H), 7.24 (d, J = 4.80 Hz, 1H), 6.79 (br s, 1H), 5.23 (s, 2H), 3.91 (s, 3H).

B. [4-(5-Methoxy-1-methyl-1,2,3,6-tetrahydropyridin-4-yl)phenyl]carbamic Acid Benzyl Ester (41). To a solution of **40** (563 mg, 1.68 mmol) in acetone (10 mL) was added iodomethane (158 μ L, 2.5 mmol). The mixture was stirred at 50 °C for 1 h then at rt overnight. The solvent was evaporated, and the residue was dissolved in ethanol (10 mL). To the solution cooled in an ice water bath was added sodium borohydride (95 mg, 2.5 mmol) portionwise. The solution was stirred at rt for 1 h. Water was added, and the reaction mixture was twice extracted with ethyl acetate (50 mL). The organic layer was dried over Na_2SO_4 and concentrated to give the title compound as a brown solid (460 mg, 81%). ^1H NMR (400 MHz, CDCl_3) δ 7.29–7.43 (m, 9H), 6.75 (br s, 1H), 5.20 (s, 2H), 3.43 (s, 3H), 3.10 (m, 2H), 2.55–2.63 (m, 2H), 2.46–2.53 (m, 2H), 2.43 (s, 3H).

C. [4-(1-Methyl-3-oxo-piperidin-4-yl)phenyl]carbamic Acid Benzyl Ester (42). To a solution of **41** (460 mg, 1.31 mmol) in THF (10 mL) was added aq HCl (6 N, 5 mL). The mixture was stirred at 50 °C for 16 h. The solvent was evaporated, and the residue was purified by flash chromatography ($\text{CH}_3\text{OH}/\text{CH}_2\text{Cl}_2$ 1:9, v/v). A white solid was obtained (300 mg, 68%). ^1H NMR (400 MHz, CDCl_3) δ 7.28–7.43 (m, 7H), 7.05 (d, J = 8.59 Hz, 2H), 6.91 (br s, 1H), 5.18 (s, 2H), 3.65 (t, J = 6.32 Hz, 0.5H), 3.56 (t, J = 6.57 Hz, 0.5H), 3.44 (t, J = 9.35 Hz, 1H), 3.27–3.35 (m, 1H), 2.95–3.04 (m, 1H), 2.85 (d, J = 13.89 Hz, 1H), 2.53 (dt, J = 7.07, 11.62 Hz, 1H), 2.38 (s, 3H), 2.16–2.25 (m, 2H), 1.81–1.91 (m, 0.5H), 1.68–1.73 (m, 0.5H).

D. [4-(3,3-Difluoro-1-methylpiperidin-4-yl)phenyl]carbamic Acid Benzyl Ester (43). To a solution of **42** (300 mg, 0.89 mmol) in CH_2Cl_2 (5 mL) cooled in an ice–water bath was added Deoxo-Fluor (50% in toluene, 1 mL, 2.7 mmol) slowly under argon. The mixture was stirred at rt overnight. Water was added, and the reaction mixture was twice extracted with CH_2Cl_2 (20 mL). The organic layer was dried over Na_2SO_4 and concentrated to a brown oil, which was purified by flash chromatography (eluted with $\text{CH}_3\text{OH}/\text{CH}_2\text{Cl}_2$ 1:9, v/v). A yellow solid was obtained (90 mg, 28%). ^1H NMR (400 MHz, CDCl_3) δ 7.36 (m, 7H), 7.25 (d, J = 8.42, 2H), 6.82 (s, 1H), 5.18 (s, 2H), 3.16 (m, 1H), 2.99 (d, J = 10.7, 1H), 2.82 (m, 1H), 2.38 (s, 3H), 2.33 (m, 2H), 1.84 (m, 1H).

E. 4-(3,3-Difluoro-1-methylpiperidin-4-yl)phenylamine (44). Compound **43** (90 mg, 0.25 mmol) was dissolved in methanol (100 mL) and the solution was passed through an H-Cube (1 mL/min, 10% Pd/C). The solvent was evaporated to leave the title compound as pale-yellow oil (45 mg, 80%). ^1H NMR (400 MHz, CD_3OD) δ 7.05 (d, J = 8.22 Hz, 2H), 6.69 (d, J = 8.61 Hz, 2H), 3.18–3.26 (m, 1H), 3.08 (d, J = 10.17 Hz, 1H), 2.83–3.02 (m, 1H), 2.49–2.65 (m, 1H), 2.47 (s, 3H), 2.39 (t, J = 12.13 Hz, 1H), 2.10–2.26 (m, 1H), 1.86 (ddd, J = 2.35, 4.70, 11.35 Hz, 1H).

F. 2-[4-(3,3-Difluoro-1-methylpiperidin-4-yl)phenylamino]-8-indan-5-yl-5-oxo-5,8-dihydropyrido[2,3-d]pyrimidine-6-carboxylic Acid Methoxyamide (38). The title compound was prepared from **24** (60 mg, 0.14 mmol) and **44** (45 mg, 0.2 mmol) using the similar procedure as described in the preparation of **29**. The title compound was obtained as a yellow solid (45.3 mg, 58%). ^1H NMR (400 MHz, $\text{CDCl}_3/\text{CD}_3\text{OD}$, 19:1, v/v) δ 9.35 (br s, 1H), 8.83 (br s, 1H), 7.42 (d, J = 7.83 Hz, 1H), 7.29 (br s, 2H), 7.26 (s, 1H), 7.17 (d, J = 7.83 Hz, 1H), 7.04 (br s, 2H), 3.89 (s, 3H), 3.12–3.25 (m, 1H), 2.92–3.11 (m, 5H), 2.71–2.92 (m, 1H), 2.41 (s, 3H), 2.26–2.39 (m, 1H), 2.10–2.26 (m, 4H), 1.79–1.91 (m, 1H). Mass spectrum (LCMS, ESI pos.) calcd for $\text{C}_{30}\text{H}_{30}\text{F}_2\text{N}_6\text{O}_3$, 561.23 (M + H); found, 561.2. HPLC: t_R = 4.65 min (100% pure).

2-[3-(1-Ethyl-3-hydroxy-piperidin-3-yl)phenylamino]-8-indan-5-yl-5-oxo-5,8-dihydropyrido[2,3-d]pyrimidine-6-carboxylic Acid Methoxyamide (39). **A. 3-(3-Aminophenyl)-1-ethylpiperidin-3-ol.**

To a solution of 1-ethylpiperidin-3-one (4 g, 31.4 mmol) in THF (40 mL) at -10°C is added dropwise 3-[bis(trimethylsilyl)amino]phenylmagnesium chloride (32 mL, 1 M in THF). The reaction was stirred for 1 h with gradual warming to rt. The mixture was then diluted with ethyl acetate, and a 0.5 M solution of aq HCl was added. The aqueous layer was washed once more with ethyl acetate and then was neutralized with sodium bicarbonate and concentrated in vacuo. The resulting solid was triturated with ethyl acetate and filtered. The filtrate was then concentrated in vacuo, and the crude was purified by flash chromatography ($\text{CH}_3\text{OH}/\text{CH}_2\text{Cl}_2$ 1:9, v/v). The title compound was obtained as yellow oil (3.7 g, 53%). ^1H NMR (400 MHz, CDCl_3) δ 6.97 (t, $J = 7.83$ Hz, 1H), 6.78 (s, 1H), 6.65 (d, $J = 8.02$ Hz, 1H), 6.45 (dd, $J = 1.56$, 8.02 Hz, 1H), 2.93 (d, 1H), 2.53 (m, 6H), 2.05 (m, 2H), 1.75 (m, 2H), 1.05 (t, $J = 7.48$, 3H).

B. 2-[3-(1-Ethyl-3-hydroxy-piperidin-3-yl)phenylamino]-8-indan-5-yl-5-oxo-5,8-dihydropyrido[2,3-d]pyrimidine-6-carboxylic Acid Methoxyamide (39). To a solution of **24** (50 mg, 0.12 mmol) in DMF/1,4 dioxane (2 mL, 1:1 v/v) was added 3-(3-aminophenyl)-1-ethylpiperidin-3-ol (42 mg, 0.144 mmol) and silver triflate (40 mg, 0.157 mmol). The mixture was stirred at 107°C for 2 h. The reaction mixture was diluted with ethyl acetate and ammonia (7 M in MeOH, 2 mL) was added. The organics were washed twice with water. The organic solvent was evaporated, and the crude was purified on prep. TLC plate (7 N ammonia in MeOH/ CH_2Cl_2 19:1, v/v) affording the title compound as a yellow solid (22 mg, 33%). ^1H NMR (400 MHz, CDCl_3) δ 9.30 (s, 1H), 8.73 (s, 1H), 7.34 (d, $J = 7.83$ Hz, 1H), 7.19 (s, 1H), 7.06 (m, 2H), 6.86 (t, $J = 2.02$ Hz, 1H), 6.75 (d, $J = 7.83$ Hz, 1H), 6.535 (dd, $J = 2.02$, 7.83 Hz, 1H), 3.82 (s, 3H), 2.99 (t, $J = 7.33$ Hz, 2H), 2.92 (t, $J = 7.33$ Hz, 2H), 2.83 (d, $J = 11.11$ Hz, 1H), 2.77 (m, 2H), 2.53 (m, 4H), 2.28 (q, $J = 6.58$ Hz, 2H), 2.15 (m, 2H), 1.66 (m, 2H), 1.05 (t, $J = 7.48$, 3H) Mass spectrum (LCMS, ESI pos.) calcd for $\text{C}_{31}\text{H}_{34}\text{N}_6\text{O}_4$, 555.26 (M + H); found, 555.1. HPLC: $t_R = 4.91$ min (100% pure).

8-(4-Ethylphenyl)-2-[4-(1-methylpiperidin-4-yl)phenylamino]-5-oxo-5,8-dihydropyrido[2,3-d]pyrimidine-6-carboxylic Acid Methoxyamide (45). 8-(4-Ethylphenyl)-2-methanesulfonyl-5-oxo-5,8-dihydropyrido[2,3-d]pyrimidine-6-carboxylic acid methoxyamide (1.5 g, 3.73 mmol, prepared similarly as **24** from the common intermediate **20**) and 4-(1-methylpiperidin-4-yl)-phenylamine (1.42 g, 7.46 mmol) in AcOH (10 mL) was heated at 110°C for 15 min. The reaction mixture was concentrated, and the remaining residue was partitioned between sat. NaHCO_3 and CH_2Cl_2 . The organic layer was dried over Na_2SO_4 , filtered, and the solvent was evaporated. MeOH (20 mL) was added, and a fine precipitate formed that was collected by filtration to provide the title compound as an off-white solid (800 mg, 42%). ^1H NMR (400 MHz, CDCl_3) δ 11.97 (s, 1H), 9.36 (s, 1H), 8.81 (s, 1H), 7.63 (br s, 1H), 7.38–7.46 (m, 2H), 7.30–7.36 (m, 2H), 7.23 (br s, 2H), 6.95 (br s, 2H), 3.90 (s, 3H), 2.97 (d, $J = 11.35$ Hz, 2H), 2.82 (q, $J = 7.56$ Hz, 2H), 2.35–2.45 (m, 1H), 2.32 (s, 3H), 1.98–2.09 (m, 2H), 1.72–1.82 (m, 4H), 1.37 (t, $J = 7.63$ Hz, 3H). Mass spectrum (LCMS, APCI pos.) calcd for $\text{C}_{29}\text{H}_{32}\text{N}_6\text{O}_3$, 513.25 (M + H); found, 513.2. HPLC: $t_R = 4.57$ min (100% pure).

8-(3-Ethylphenyl)-2-[4-(1-methylpiperidin-4-yl)phenylamino]-5-oxo-5,8-dihydropyrido[2,3-d]pyrimidine-6-carboxylic Acid Methoxyamide (46). Using a similar procedure described in the preparation of **45**, the title compound was obtained as a yellow solid (34.8 mg, 67%). ^1H NMR (400 MHz, CDCl_3) δ 11.98 (s, 1H), 9.36 (s, 1H), 8.82 (s, 1H), 7.66 (br s, 1H), 7.42–7.55 (m, 2H), 7.17–7.26 (m, 4H), 6.94 (br s, 2H), 3.90 (s, 3H), 3.08 (d, $J = 10.17$ Hz, 2H), 2.75 (q, $J = 7.43$ Hz, 2H), 2.41 (m, 4H), 2.15 (br s, 2H), 1.80 (br s, 4H), 1.27 (t, $J = 7.63$ Hz, 3H). Mass spectrum (LCMS, APCI pos.) calcd for $\text{C}_{29}\text{H}_{32}\text{N}_6\text{O}_3$, 513.25 (M + H); found, 513.2. HPLC: $t_R = 4.53$ min (100% pure).

8-(6,7-Dihydro-5H-[1]pyrindin-3-yl)-2-[4-(1-methylpiperidin-4-yl)phenylamino]-5-oxo-5,8-dihydropyrido[2,3-d]pyrimidine-6-carboxylic Acid Methoxyamide (47). 8-(6,7-Dihydro-5H-[1]pyrindin-3-yl)-2-methanesulfonyl-5-oxo-5,8-dihydropyrido[2,3-d]pyrimidine-6-carboxylic acid methoxyamide (30 mg, 0.07 mmol), prepared similarly to **24** from the common intermediate **20** and 6,7-dihydro-

5H-[1]pyrindin-3-ylamine⁴⁰) and 4-(1-methylpiperidin-4-yl)-phenylamine (20 mg, 0.1 mmol) in AcOH (1 mL) was heated at 110°C for 10 min. The reaction mixture was concentrated, and the remaining residue was partitioned between sat. NaHCO_3 and CH_2Cl_2 . The organic layer was dried over Na_2SO_4 , filtered, and the solvent was evaporated. The residue was purified by preparative HPLC ($\text{MeCN}/\text{H}_2\text{O}$ 1:10 to 10:1, v/v, linear gradient over 12 min). A yellow solid was obtained (7.3 mg, 20%). ^1H NMR (400 MHz, CDCl_3) δ 11.89 (s, 1H), 9.38 (s, 1H), 8.76 (s, 1H), 8.38–8.52 (m, 1H), 7.57 (s, 1H), 7.23 (br s, 2H), 7.00 (br s, 2H), 3.90 (s, 3H), 3.19 (t, $J = 7.63$ Hz, 2H), 3.05 (t, $J = 7.43$ Hz, 2H), 2.98 (d, $J = 11.35$ Hz, 2H), 2.42 (m, 1H), 2.24–2.36 (m, 5H), 2.04 (td, $J = 2.93$, 11.44 Hz, 2H), 1.64–1.86 (m, 4H). Mass spectrum (LCMS, APCI pos.) calcd for $\text{C}_{29}\text{H}_{31}\text{N}_7\text{O}_3$, 526.25 (M + H); found, 526.3. HPLC: $t_R = 3.94$ min (100% pure).

8-(4,4-Dimethylcyclohexyl)-2-[4-(1-methylpiperidin-4-yl)phenylamino]-5-oxo-5,8-dihydropyrido[2,3-d]pyrimidine-6-carboxylic Acid Methoxyamide (48). Using a similar procedure described in the preparation of **47**, the title compound was obtained as a yellow solid (25.9 mg, 43%). ^1H NMR (400 MHz, CDCl_3) δ 12.02 (s, 1H), 9.36 (s, 1H), 8.82 (s, 1H), 7.68 (br s, 1H), 7.55 (d, $J = 8.61$ Hz, 2H), 7.25 (d, $J = 7.04$ Hz, 2H), 4.98–5.14 (m, 1H), 3.88 (s, 3H), 3.05 (d, $J = 10.96$ Hz, 2H), 2.53 (quin, $J = 7.83$ Hz, 1H), 2.37 (s, 3H), 2.06–2.22 (m, 2H), 1.83–2.03 (m, 8H), 1.66 (d, $J = 13.30$ Hz, 2H), 1.39–1.56 (m, 2H), 1.06 (s, 3H), 1.04 (s, 3H). Mass spectrum (LCMS, APCI pos.) calcd for $\text{C}_{29}\text{H}_{38}\text{N}_6\text{O}_3$, 519.30 (M + H); found, 519.2. HPLC: $t_R = 4.83$ min (100% pure).

8-Cyclohexyl-2-[4-(1-methylpiperidin-4-yl)phenylamino]-5-oxo-5,8-dihydropyrido[2,3-d]pyrimidine-6-carboxylic Acid Methoxyamide (49). Using a similar procedure described in the preparation of **47**, the title compound was obtained as a yellow solid (34 mg, 38%). ^1H NMR (400 MHz, CDCl_3) δ 12.00 (s, 1H), 9.37 (s, 1H), 8.81 (s, 1H), 7.53–7.65 (m, $J = 8.22$ Hz, 2H), 7.20–7.25 (m, $J = 8.61$ Hz, 2H), 5.16 (t, $J = 11.93$ Hz, 1H), 3.89 (s, 3H), 3.10–3.28 (m, 1H), 2.72–2.84 (m, 1H), 2.58–2.70 (m, 1H), 2.33 (s, 3H), 1.99–2.12 (m, 5H), 1.72–1.97 (m, 5H), 1.47–1.71 (m, 4H), 1.21–1.39 (m, 2H). Mass spectrum (LCMS, APCI pos.) calcd for $\text{C}_{27}\text{H}_{34}\text{N}_6\text{O}_3$, 491.27 (M + H); found, 491.2. HPLC: $t_R = 4.37$ min (100% pure).

Biology. Kinase Assays. Assays for FMS and the other kinases listed in Table 5 were carried out using a fluorescence polarization competition immunoassay format and have been described elsewhere in detail.^{23b} The full cytoplasmic regions of FMS (538–972) encompassing the tyrosine kinase domain was expressed and purified from a baculovirus system.²⁹ The FMS kinase assay measured FMS-mediated phosphorylation of tyrosine residues present on a synthetic FMS_{555–568} peptide (SYEGNSYTFIDPTQ). To each well of a black 96-well microplate (cat. no. 42-000-0117, Molecular Devices, Sunnyvale, CA), Then 5 μL of compound (in 4% DMSO) were mixed with 2 μL of 3.5 nM FMS, 25 mM MgCl_2 in assay buffer (100 mM HEPES, pH 7.5, 1 mM DTT, 0.01% Tween-20), and 2 μL of 1540 μM peptide in assay buffer. The kinase reaction was initiated by adding 1 μL of 10 mM ATP in assay buffer. Final concentrations in the 10 μL reaction mixture were 100 mM HEPES, pH 7.5, 1 mM DTT, 0.01% Tween-20, 2% DMSO, 308 μM SYEGNSYTFIDPTQ, 1 mM ATP, 5 mM MgCl_2 , and 0.7 nM FMS. The plates were incubated at room temperature for 80 min. Reactions were stopped by addition of 1.2 μL of 50 mM EDTA. Each well then received 10 μL of a 1:1:3 mixture of 10 \times antiphosphotyrosine antibody, 10 \times PTK green tracer, and fluorescence polarization dilution buffer (cat. no. P2837, Invitrogen, Carlsbad, CA). The plates were incubated for 30 min at room temperature, and the fluorescence polarization was read (485 nm excitation, 530 nm emission) on an Analyst plate reader (Molecular Devices). Fluorescence polarization values for positive (EDTA) and negative (DMSO) controls were approximately 290 and 160, respectively, and were used to define 100% and 0% inhibition of the FMS reaction.

Bone Marrow-Derived Macrophage (BMDM) Proliferation Assay. Functional impact on cellular FMS activity was determined by measuring compound inhibition of CSF-1-driven proliferation

of mouse bone marrow-derived macrophages as previously described.²⁹ Macrophages were derived by culturing mouse bone marrow in α -MEM supplemented with 10% FCS and 50 ng/mL recombinant mouse CSF-1 in bacteriologic dishes. On the sixth day, macrophages were resuspended to 50000 cells/mL in α -MEM containing 10% FCS, and 100 μ L of cell suspension were distributed per well into 96-well culture plates for overnight culture. Next, wells were further supplemented with the addition of 50 μ L media containing 15 ng/mL CSF-1, 3 μ M indomethacin, and a dilution series of test compound. The cells were cultured for 30 h at 37 °C and 5% CO₂. During the final 6 h, cultures were supplemented with an additional 30 μ L of media containing a 1:500 dilution of bromodeoxyuridine (BrDU) reagent, and incorporation of BrDU into cellular DNA was quantified using a specific ELISA (cat. no. X1327K) from Exalpha Corporation (Watertown, MA).

MV-4-11 and M-07e Leukemia Cell Line Proliferation Assays. Functional impact on cellular FLT3 activity was determined by measuring compound inhibition of MV-4-11 (ATCC no.: CRL-9591) cell proliferation, and M-07e (DSMZ no.: ACC 104) cells were used to assess compound effects on cellular KIT activity. MV-4-11 cells grew independent of growth factor due to expression of a constitutive active FLT3 mutation, and M-07e cells were driven to proliferate in a KIT-dependent fashion by 25 ng/mL stem cell factor. Following a culture period of 72 h, relative cell numbers were determined using CellTiterGlo reagent (Promega).

Biochemical Pharmacodynamic Mouse Model. Groups of six B6C3F1 mice (Taconic Farms), 8 weeks of age, were given oral doses of vehicle (aq 20% hydroxypropyl- β -cyclodextrin (HP β CD)) or **37** at 1 or 3 mg/kg. Six hours later, mice were administered saline alone or saline containing 1 μ g of recombinant mouse CSF-1 (Cell Biosciences Inc., Norwood, MA) via the tail vein. Fifteen minutes after CSF-1 injection, mice were sacrificed and spleens were isolated and snap frozen on dry ice. The frozen tissue was homogenized in 1 mL of Trizol (Invitrogen) per 50 mg of tissue, and RNA was purified according to the Trizol instructions and treated with 6.8 Kunitz units of RNase-free DNase (Qiagen, Valencia, CA) to degrade contaminating genomic DNA. The RNA was purified further using RNeasy columns (Qiagen). RT-PCR was performed in 25 μ L reaction volumes using Reverse Transcriptase qPCR Master Mix (Eurogentec) and approximately 50 ng of RNA. Applied Biosystems, Inc., (Foster City, CA) was the source for the primers and probes for mouse c-fos mRNA (cat. no. Mm00487425) and 18S rRNA (cat. no. 4333760F). Amplification and detection were performed using an ABI Prism 7900. Standard curves were created for c-fos mRNA and for 18S rRNA using RNA isolated from a vehicle-treated, CSF-1-induced mouse and used to calculate relative expression levels in all other samples. c-fos mRNA values were normalized to 18S rRNA content. Averaged, normalized c-fos content in the saline (no CSF-1) group was assigned a value of one and all other groups were expressed as "fold-induced".

SCW-Induced Arthritis Model. Female Lewis rats (80–100 g each) were purchased from Charles River. Streptococcal cell wall peptidoglycan–polysaccharide polymers (PG-PS 10S) were purchased from BD (cat. no. 210866). On day 0, rats were anesthetized using isoflurane and injected ip with PG-PS 10S equivalent to 15 μ g of rhamnose/gram (body weight) in the lower left quadrant of the abdomen. Control rats were treated in a similar manner with sterile saline. On day 5, rats were injected with PG-PS 10S, and those that showed a distinct acute phase arthritic response based on joint swelling were randomized into the treatment groups. A chronic, T cell dependent, erosive arthritis begins in this model on about day 10. Animals were dosed orally twice a day beginning on day 19. Compound **37** was formulated in 20% HP β CD. The dose volume was 6 mL/kg. Left and right hind ankles of each rat were measured with calipers every day for the first six days (postinjection) and then at least every two or three days for the remainder of the study.

Adjuvant-Induced Arthritis Model. The adjuvant-induced arthritis study was performed by Bolder BioPath, Inc., (Boulder, CO). Male Lewis rats (Harlan Cat. no. 1439444), 165–185 g, were anesthetized with isoflurane and injected with 100 μ L of Freund's

complete adjuvant (FCA, Sigma)/lipoidal amine (LA, Sigma) at the base of the tail on day 0. Oral dosing was initiated on day 8 (the first day of clinical disease). Compound **37** or vehicle (20% HP β CD) were dosed orally twice daily. Caliper measurements of ankles were taken on days 7–21. To calculate the area under the curve (AUC), the daily caliper measurements for each rat were integrated vs time (treatment day). Mean AUC values for each group were determined, and the percent inhibition from arthritis vehicle-treated controls was calculated after subtracting the AUC of age-matched normal control animals. Following necropsy on day 21, digital radiographs of left paws were prepared using a VetTek Universal AP500 (Del Medical Imaging Corporation, Franklin Park, IL). Both hind paws were then fixed in formalin and processed for H and E microscopy. H and E sections were scored for bone resorption as follows: 0 = normal; 0.5 = normal on low magnification but have the earliest hint of small areas of resorption in the metaphysis with no resorption in the tarsal bones; 1 = (minimal) small definite areas of resorption in distal tibial trabecular or cortical bone, or in the tarsal bones, not readily apparent on low magnification, rare osteoclasts; 2 = (mild) more numerous areas ($\leq 25\%$ loss of bone in growth plate area) of resorption in distal tibial trabecular or cortical bone and tarsals apparent on low magnification, osteoclasts more numerous; 3 = (moderate) obvious resorption of medullary trabecular and cortical bone without full thickness defects in both distal tibial cortices, loss of some medullary trabeculae with 26–50% loss across growth plate and cortices, some loss in tarsal bones, lesion apparent on low magnification, osteoclasts more numerous; 4 = (marked) full or near full thickness defects in both distal tibial cortices, often with distortion of profile of remaining cortical surface, marked loss of medullary bone of distal tibia (50–100% loss across growth plate area and cortices and up to 50% loss in small tarsals if minor in tibia), numerous osteoclasts, minor to mild resorption in smaller tarsal bones; 5 = (severe) full thickness defects in both distal tibial cortices with $> 75\%$ loss across growth plate and both cortices and $> 50\%$ loss in tarsals, often with distortion of profile of remaining cortical surface, marked loss of medullary bone of distal tibia, numerous osteoclasts. Osteoclast counts (5, 400 \times fields) were performed on ankles in the areas of greatest bone resorption.

Statistical Analysis. Ankle thickness, bone erosion scores, osteoclast counts, and c-fos expression values (mean \pm SE) were analyzed for group differences using the Student's *t* test. Significance was set at $p \leq 0.05$.

Supporting Information Available: LC-MS data for target compounds. This material is available free of charge via the Internet at <http://pubs.acs.org>.

References

- (1) (a) Sacca, R.; Stanley, E. R.; Sherr, C. J.; Rettenmier, C. W. Specific binding of the mononuclear phagocyte colony-stimulating factor CSF-1 to the product of the v-fms oncogene. *Proc. Natl. Acad. Sci. U.S.A.* **1986**, *83*, 3331–3335. (b) Pixley, F. J.; Stanley, E. R. CSF-1 Regulation of the wandering macrophage: complexity in action. *Trends Cell Biol.* **2004**, *14*, 628–638.
- (2) Wiktor-Jedrzejczak, W.; Ahmed, A.; Szczylik, C.; Skelly, R. R. Hematological characterization of congenital osteopetrosis in op/op mouse. *J. Exp. Med.* **1982**, *156*, 1516–1527.
- (3) Pollard, J. W.; Stanley, E. R. Pleiotropic roles for CSF-1 in development defined by the mouse mutation osteopetrotic (op). *Adv. Dev. Biochem.* **1995**, *4*, 153–193.
- (4) MacDonald, K. P. A.; Rowe, V.; Bofinger, H. M.; Thomas, R.; Sasmono, T.; Hume, D. A.; Hill, G. R. The colony-stimulating factor 1 receptor is expressed on dendritic cells during differentiation and regulates their expansion. *J. Immunol.* **2005**, *175*, 1399–1405.
- (5) Pixley, F. J.; Stanley, E. R. CSF-1 regulation of the wandering macrophage: complexity in action. *Trends Cell Biol.* **2004**, *14*, 628–638.
- (6) Park, Y.; Ahn, C.; Choi, H. K.; Lee, S.; In, B.; Lee, H.; Nam, C.; Lee, S. Atherosclerosis in rheumatoid arthritis: morphologic evidence obtained by carotid ultrasound. *Arthritis Rheum.* **2002**, *46*, 1714–1719.
- (7) Joffe, I.; Epstein, S. Osteoporosis associated with rheumatoid arthritis: pathogenesis and management. *Semin. Arthritis Rheum.* **1991**, *20*, 256–272.

- (8) Lipsky, P. E.; Van Der Heijde, D. M. F. M.; St. Clair, E. W.; Furst, D. E.; Breedveld, F. C.; Kalden, J. R.; Smolen, J. S.; Weisman, M.; Emery, P.; Feldmann, M.; Harriman, G. R.; Maini, R. N. Infliximab and methotrexate in the treatment of rheumatoid arthritis. *N. Engl. J. Med.* **2000**, *343*, 1594–602.
- (9) Borchers, A. T.; Keen, C. L.; Cheema, G. S.; Gershwin, M. E. The use of methotrexate in rheumatoid arthritis. *Semin. Arthritis Rheum.* **2004**, *34*, 465–483.
- (10) (a) Kawaji, H.; Yokomuro, K.; Kikuchi, K.; Somoto, Y.; Shirai, Y. Macrophage colony-stimulating factor in patients with rheumatoid arthritis. *Nippon Ika Daigaku Zasshi* **1995**, *62*, 260–270. (b) Ritchlin, C.; Dwyer, E.; Bucala, R.; Winchester, R. Sustained and distinctive patterns of gene activation in synovial fibroblasts and whole synovial tissue obtained from inflammatory synovitis. *Scand. J. Immunol.* **1994**, *40*, 292–298. (c) Takei, I.; Takagi, M.; Ida, H.; Ogino, T.; Santavirta, S.; Kontinen, Y. T. High macrophage-colony stimulating factor levels in synovial fluid of loose artificial hip joints. *J. Rheumatol.* **2000**, *27*, 894–899.
- (11) Shinohara, S.; Hirohata, S.; Inoue, T.; Ito, K. Phenotypic analysis of peripheral blood monocytes isolated from patients with rheumatoid arthritis. *J. Rheumatol.* **1992**, *19*, 211–215.
- (12) Weiner, L. M.; Li, W.; Holmes, M.; Catalano, R. B.; Dohnansky, M.; Padavic, K.; Alpaugh, R. K. Phase I trial of recombinant macrophage colony-stimulating factor and recombinant gamma-interferon: toxicity, monocytosis, and clinical effects. *Cancer Res.* **1994**, *54*, 4084–4090.
- (13) Hanamura, T.; Asakura, E.; Tanabe, T. Macrophage colony-stimulating factor (CSF-1) augments cytokine induction by lipopolysaccharide (LPS)-stimulation and by bacterial infections in mice. *Immunopharmacology* **1997**, *37*, 15–23.
- (14) Hamilton, J. A. Rheumatoid arthritis: opposing actions of haemopoietic growth factors and slow-acting anti-rheumatic drugs. *Lancet* **1993**, *342*, 536–539.
- (15) (a) Castro-Rueda, H.; Kavanaugh, A. Biologic therapy for early rheumatoid arthritis: the latest evidence. *Curr. Opin. Rheumatol.* **2008**, *20*, 314–9. (b) Ilowite, N. T. Update on biologics in juvenile idiopathic arthritis. *Curr. Opin. Rheumatol.* **2008**, *20*, 613–618. (c) Kitaura, H.; Zhou, P.; Kim, H.; Novack, D. V.; Ross, F. P.; Teitelbaum, S. L. M-CSF mediates TNF-induced inflammatory osteolysis. *J. Clin. Invest.* **2005**, *115*, 3418–3427.
- (16) (a) Uemura, Y.; Ohno, H.; Ohzeki, Y.; Takanashi, H.; Murooka, H.; Kubo, K.; Serizawa, I. The selective M-CSF receptor tyrosine kinase inhibitor Ki20227 suppresses experimental autoimmune encephalomyelitis. *J. Neuroimmunol.* **2008**, *195*, 73–80. (b) Ohno, H.; Uemura, Y.; Murooka, H.; Takanashi, H.; Tokieda, T.; Ohzeki, Y.; Kubo, K.; Serizawa, I. The orally-active and selective c-FMS tyrosine kinase inhibitor Ki20227 inhibits disease progression in a collagen-induced arthritis mouse model. *Eur. J. Immunol.* **2008**, *38*, 283–291.
- (17) Conway, J. G.; McDonald, B.; Parham, J.; Keith, B.; Rusnak, D. W.; Shaw, E.; Jansen, M.; Lin, P.; Payne, A.; Crosby, R. M.; Johnson, J. H.; Frick, L.; Lin, M. J.; Depee, S.; Tadepalli, S.; Votta, B.; James, I.; Fuller, K.; Chambers, T. J.; Kull, F. C.; Chamberlain, S. D.; Hutchins, J. T. Inhibition of colony-stimulating-factor-1 signaling in vivo with the orally bioavailable cFMS kinase inhibitor GW2580. *Proc. Nat. Acad. Sci. U.S.A.* **2005**, *102*, 16078–16083. (b) Conway, J. G.; Pink, H.; Bergquist, M. L.; Han, B.; Depee, S.; Tadepalli, S.; Lin, P.; Crumrine, R. C.; Binz, J.; Clark, R. L.; Selph, J. L.; Stimpson, S. A.; Hutchins, T. J.; Chamberlain, S. D.; Brodie, T. A. Effects of the cFMS kinase inhibitor 5-(3-methoxy-4-((4-methoxybenzyl)oxy)benzyl)pyrimidine-2,4-diamine (GW2580) in normal and arthritic rats. *J. Pharmacol. Exp. Ther.* **2008**, *326*, 41–50.
- (18) Ibrahim, P. N.; Artis, D. R.; Bremer, R.; Habets, G.; Mamo, S.; Nespi, M.; Zhang, C.; Zhang, J.; Zhu, Y.; Zuckerman, R.; West, B.; Suzuki, Y.; Tsai, J.; Hirth, K.-P.; Bollag, G.; Spevak, W.; Cho, H.; Gillette, S. J.; Wu, G.; Zhu, H.; Shi, S. Pyrrolo[2,3-*b*]pyridine derivatives as protein kinase inhibitors and their preparation, pharmaceutical compositions and use in the treatment of diseases. PCT Int. Appl. WO 2007002433, 2007.
- (19) Ajami, A. M.; Boss, M. A.; Paterson, J. Treatment of autoimmune and demyelinating diseases with Symadex and related imidazoacridine derivatives. PCT Int. Appl. WO 2006081431, 2006.
- (20) Patyna, S.; Laird, A. D.; Mendel, D. B.; O'Farrell, A.; Liang, C.; Guan, H.; Vojkovsky, T.; Vasile, S.; Wang, X.; Chen, J.; Grazzini, M.; Yang, C. Y.; Haznedar, J. O.; Sukbuntherng, J.; Zhong, W.; Cherrington, J. M.; Hu-Lowe, D. SU14813: a novel multiple receptor tyrosine kinase inhibitor with potent antiangiogenic and antitumor activity. *Mol. Cancer Ther.* **2006**, *5*, 1774–1782.
- (21) Tamaskar, I.; Garcia, J. A.; Elson, P.; Wood, L.; Mekhail, T.; Dreicer, R.; Rini, B. I.; Bukowski, R. M. Antitumor effects of sunitinib or sorafenib in patients with metastatic renal cell carcinoma who received prior antiangiogenic therapy. *J. Urol.* **2008**, *179*, 81–86.
- (22) Guo, J.; Marcotte, P. A.; McCall, J. O.; Dai, Y.; Pease, L. J.; Michaelides, M. R.; Davidsen, S. K.; Glaser, K. B. Inhibition of phosphorylation of the colony-stimulating factor-1 receptor (c-FMS) tyrosine kinase in transfected cells by ABT-869 and other tyrosine kinase inhibitors. *Mol. Cancer Ther.* **2006**, *5*, 1007–1013.
- (23) (a) Patch, R. J.; Brandt, B. M.; Asgari, D.; Baidur, N.; Chadha, N. K.; Georgiadis, T.; Cheung, W. S.; Petrounia, I. P.; Donatelli, R. R.; Chaikin, M. A.; Player, M. R. Potent 2'-aminoanilide inhibitors of cFMS as potential anti-inflammatory agents. *Bioorg. Med. Chem. Lett.* **2007**, *17*, 6070–6074. (b) Illig, C. R.; Chen, J.; Wall, M. J.; Wilson, K. J.; Ballentine, S. K.; Rudolph, M. J.; DesJarlais, R. L.; Chen, Y.; Schubert, C.; Petrounia, I.; Crysler, C. S.; Molloy, C. J.; Chaikin, M. A.; Manthey, C. L.; Player, M. R.; Tomczuk, B. E.; Meegalla, S. K. Discovery of novel FMS kinase inhibitors as anti-inflammatory agents. *Bioorg. Med. Chem. Lett.* **2008**, *18*, 1642–1648. (c) Meegalla, S. K.; Wall, M. J.; Chen, J.; Wilson, K. J.; Ballentine, S. K.; DesJarlais, R. L.; Schubert, C.; Crysler, C. S.; Chen, Y.; Molloy, C. J.; Chaikin, M. A.; Manthey, C. L.; Player, M. R.; Tomczuk, B. E.; Illig, C. R. Structure-based optimization of a potent class of arylamide FMS inhibitors. *Bioorg. Med. Chem. Lett.* **2008**, *18*, 3632–3637.
- (24) Wall, M. J.; Chen, J.; Meegalla, S. K.; Ballentine, S. K.; Wilson, K. J.; DesJarlais, R. L.; Schubert, C.; Chaikin, M. A.; Crysler, C.; Petrounia, I. P.; Donatelli, R. R.; Yurkow, E. J.; Boczon, L.; Mazzulla, M.; Player, M. R.; Patch, R. J.; Manthey, C. L.; Molloy, C.; Tomczuk, B. E.; Illig, C. R. Synthesis and evaluation of novel 3,4,6-substituted 2-quinolones as FMS kinase inhibitors. *Bioorg. Med. Chem. Lett.* **2008**, *18*, 2097–2102.
- (25) Huang, H.; Hutta, D. A.; Hu, H.; DesJarlais, R. L.; Schubert, C.; Petrounia, I. P.; Chaikin, M. A.; Manthey, C. L.; Player, M. R. Design and Synthesis of a Pyrido[2,3-*d*]pyrimidin-5-one Class of Anti-inflammatory FMS Inhibitors. *Bioorg. Med. Chem. Lett.* **2008**, *18*, 2355–2361.
- (26) Pesson, M.; Antoine, M.; Chabassier, S.; Geiger, S.; Girard, P.; Richer, D.; De Lajudie, P.; Horvath, E.; Leriche, B.; Patte, S. Antibacterial derivatives of 8-alkyl-5-oxo-5,8-dihydropyrido[2,3-*d*]pyrimidine-6-carboxylic acids. I. New procedure of preparation. *Eur. J. Med. Chem.* **1974**, *9*, 585–590.
- (27) Tomita, K.; Tsuzuki, Y.; Shibamori, K.; Tashima, M.; Kajikawa, F.; Sato, Y.; Kashimoto, S.; Chiba, K.; Hino, K. Synthesis and structure-activity relationships of novel 7-substituted 1,4-dihydro-4-oxo-1-(2-thiazolyl)-1,8-naphthyridine-3-carboxylic acids as antitumor Agents. Part 1. *J. Med. Chem.* **2002**, *45*, 5564–5575.
- (28) Ruesdale, L. K.; Sherbine, J. P.; Vanasse, B. J. Preparation of 2,4-dihydroxypyridine and 2,4-dihydroxy-3-nitropyridine and nucleoside derivatives useful for treating cardiovascular diseases. PCT Int. Appl. WO9724327A1, 1997.
- (29) Schalk-Hihi, C.; Ma, H. C.; Struble, G. T.; Bayoumy, S.; Williams, R.; Devine, E.; Petrounia, I. P.; Mezzasalma, T.; Zeng, L.; Schubert, C.; Grasperger, B.; Springer, B. A.; Deckman, I. C. Protein engineering of the colony-stimulating factor-1 receptor kinase domain for structural studies. *J. Biol. Chem.* **2007**, *282*, 4085.
- (30) Schubert, C.; Schalk-Hihi, C.; Struble, G. T.; Ma, H. C.; Petrounia, I. P.; Brandt, B.; Deckman, I. C.; Patch, R. J.; Player, M. R.; Spurlino, J. C.; Springer, B. A. Crystal Structure of the Tyrosine Kinase Domain of Colony-stimulating Factor-1 Receptor (cFMS) in Complex with Two Inhibitors. *J. Biol. Chem.* **2007**, *282*, 4094 (PDB: 210Y).
- (31) The Cerep high-throughput profile consists of a broad collection of 50 transmembrane and soluble receptors, ion channels, and monoamine transporters. It has been specifically designed to provide information not only on potential limitations or liabilities of drug candidates, but also for off-target activity identification. For the test compounds, the results are expressed as a percent inhibition of control specific binding (mean values, $n = 2$).
- (32) Swindell, C. S.; Duffy, R. H. A Useful Construction of 4-Substituted 1-Alkylpiperid-3-ones. *Heterocycles* **1986**, *24*, 3373–3377.
- (33) (a) Ratajczak, M. Z.; Luger, S. M.; Gerwitz, A. M. The c-kit proto-oncogene in normal and malignant human hematopoiesis. *Int. J. Cell Cloning* **1992**, *10*, 205–214. (b) Smolich, B. D.; Yuen, H. A.; West, K. A.; Giles, F. J.; Albitar, M.; Cherrington, J. M. The antiangiogenic protein kinase inhibitors SU5416 and SU6668 inhibit the SCF receptor (c-kit) in a human myeloid leukemia cell line and in acute myeloid leukemia blasts. *Blood* **2001**, *97*, 1413–1421.
- (34) (a) Geissler, E. N.; Ryan, M. A.; Housman, D. E. The dominant-white spotting (W) locus of the mouse encodes the c-kit proto-oncogene. *Cell* **1988**, *55*, 185–192. (b) Bijangi-Vishehsaraei, K.; Saadatzaheh, M. R.; Werne, A.; McKenzie, K. A. W.; Kapur, R.; Ichijo, H.; Haneline, L. S. Enhanced TNF- α -induced apoptosis in Fanconi anemia type C-deficient cells is dependent on apoptosis signal-regulating kinase 1. *Blood* **2005**, *106*, 4124–4130.
- (35) Orloffsky, A.; Stanley, E. R. CSF 1-induced gene expression in macrophages: dissociation from the mitogenic response. *EMBO J.* **1987**, *6*, 2947–2952.

- (36) Chan, J. M. K.; Villarreal, G.; Jin, W. W.; Stepan, T.; Burstein, H.; Wahl, S. M. Intraarticular gene transfer of TNFR: Fc suppresses experimental arthritis with reduced systemic distribution of the gene product. *Mol. Ther.* **2002**, *6*, 727–736.
- (37) Cromartie, W. J.; Craddock, J. G.; Schwab, J. H.; Anderlie, S. K.; Yang, C. H. Arthritis in rats after systemic injection of streptococcal cells or cell walls. *J. Exp. Med.* **1977**, *146*, 1585–1602.
- (38) Richards, P. J.; Williams, B. D.; Williams, A. S. Suppression of chronic streptococcal cell wall-induced arthritis in lewis rats by liposomal clodronate. *Rheumatology* **2001**, *40*, 978–987.
- (39) (a) Tak, P. P.; Smeets, T. J.; Daha, M. R.; Kluin, P. M.; Meijers, K. A.; Brand, R.; Meinders, A. E.; Breedveld, F. C. Analysis of the synovial cell infiltrate in early rheumatoid synovial tissue in relation to disease activity. *Arthritis Rheum.* **1997**, *40*, 217–225. (b) Haringman, J. J.; Gerlag, D. M.; Zwinderman, A. H.; Smeets, T. J. M.; Kraan, M. C.; Baeten, D.; McInnes, I. B.; Bresnihan, B.; Tak, P. P. Synovial tissue macrophages: a sensitive biomarker for response to treatment in patients with rheumatoid arthritis. *Ann. Rheum. Dis.* **2005**, *64*, 834–838.
- (40) DAI, x. m.; Ryan, G. R.; Hapel, A. J.; Dominguez, M. G.; Russell, R. G.; Kapp, S.; Sylvestre, V.; Stanley, E. R. Targeted disruption of the mouse colony-stimulating factor 1 receptor gene results in osteopetrosis, mononuclear phagocyte deficiency, increased primitive progenitor cell frequencies, and reproductive defects. *Blood* **2002**, *99*, 111–120.
- (41) Campbell, I. K.; Rich, M. J.; Bischof, R. J.; Hamilton, J. A. The colony-stimulating factors and collagen-induced arthritis: exacerbation of disease by CSF-1 and G-CSF and requirement for endogenous CSF-1. *J. Leukocyte Biol.* **2000**, *68*, 144–50.
- (42) Tohda, Y.; Eiraku, M.; Nakagawa, T.; Usami, Y.; Ariga, M.; Kawashima, T.; Tani, K.; Watanabe, H.; Mori, Y. Nucleophilic reaction upon electron-deficient pyridone derivatives. X. One-pot synthesis of 3-nitropyridines by ring transformation of 1-methyl-3,5-dinitro-2-pyridone with ketones or aldehydes in the presence of ammonia. *Bull. Chem. Soc. Jpn.* **1990**, *63*, 2820–2827.

JM801406H